

THE UNIVERSITY OF MICHIGAN
INDUSTRY PROGRAM OF THE COLLEGE OF ENGINEERING

THE EFFECT OF MINOR LOSSES ON WATERHAMMER PRESSURE WAVES

Dinshaw M. Contractor

A dissertation submitted in partial fulfillment
of the requirements for the degree of
Doctor of Philosophy in the
University of Michigan
Department of Civil Engineering

December, 1963

IP-651

en gn

UMRC687

ACKNOWLEDGEMENTS

The author is extremely grateful to Professor Victor L. Streeter, chairman of the committee, for suggesting this interesting topic. The discussions held with him about various aspects of the thesis never failed to encourage the author in the solution of the problem. The other members of the committee are also to be thanked for their guidance and their cooperation.

The author acknowledges the financial help given him by the University of Michigan by way of a fellowship for two academic years. The funds for this work were jointly borne by the Civil Engineering Department and a National Science Foundation research project directed by Professor V. L. Streeter. Since the computer was used for the theoretical solution of the problem, the author thanks the University of Michigan Computing Center for the use of this facility.

The author is grateful to many of his colleagues with whom he has had stimulating discussions of the problem. The Industry Program has been very helpful for the typing and assembly of the thesis and the author acknowledges his indebtedness to the College of Engineering for this aid.

TABLE OF CONTENTS

	<u>Page</u>
ACKNOWLEDGEMENTS.....	ii
LIST OF FIGURES.....	iv
LIST OF PLATES.....	vi
NOMENCLATURE.....	vii
I HISTORICAL REVIEW.....	1
II INTRODUCTION.....	3
III ELEMENTARY SOLUTION.....	5
Derivation.....	6
IV SOLUTION BY THE METHOD OF CHARACTERISTICS.....	13
Derivation of Characteristic Equations.....	14
Finite-Difference Equations.....	18
V EXPERIMENTAL SET-UP.....	32
VI EXPERIMENTAL PROCEDURE.....	44
VII THE COMPUTER PROGRAM.....	47
VIII DISCUSSION OF RESULTS.....	49
IX CONCLUSIONS.....	71
APPENDIX I - COMPUTER PROGRAM AND PRINT OUT FOR WATER HAMMER IN A PIPELINE WITH A MINOR LOSS IN THE MIDDLE.....	72
APPENDIX II - COMPUTER PROGRAM AND PRINT OUT OF WATER HAMMER IN A STRAIGHT PIPELINE.....	77
BIBLIOGRAPHY.....	82

LIST OF FIGURES

<u>Figure</u>		<u>Page</u>
1	Conditions Before and After a Water-Hammer Pressure Wave Encounters a Minor Loss.....	7
2	Characteristics.....	21
3	Specified Time-Interval Method.....	21
4	The (x,t) Plane for a Uniform Pipe.....	22
5	The (x,t) Plane for a Left-Hand Boundary Condition....	22
6	The (x,t) Plane for a Right-Hand Boundary Condition...	26
7	The (x,t) Plane for a Minor Loss Boundary Condition...	26
8	The (x,t) Plane for a Valve as a Right-Hand Boundary Condition.....	31
9	Schematic Diagram of Experimental Set-Up.....	33
10	Three Orifices Used in Producing Energy Loss.....	34
11	Variation of K versus R of Three Closely-Spaced Orifices.....	35
12	Resistance of Solenoid Valve During Closure.....	38
13	Flow Diagram for Computer Program.....	48
14	Water-Hammer Pressure-Time Diagram; Case 1(a); One Cycle.....	59
15	Water-Hammer Pressure-Time Diagram; Case 1(a); Four Cycles.....	60
16	Water-Hammer Pressure-Time Diagram; Case 1(b); One Cycle.....	61
17	Water-Hammer Pressure-Time Diagram; Case 1(b); Four Cycles.....	62
18	Water-Hammer Pressure-Time Diagram; Case 1(c).....	63
19	Water-Hammer Pressure-Time Diagram; Case 1(d).....	64

LIST OF FIGURES (CONT'D)

<u>Figure</u>		<u>Page</u>
20	Water-Hammer Pressure-Time Diagram; Case 2(a).....	65
21	Water-Hammer Pressure-Time Diagram; Case 2(b).....	66
22	Water-Hammer Pressure-Time Diagram; Case 2(c).....	67

LIST OF PLATES

<u>Plate</u>		<u>Page</u>
I	Compression Chamber and Air Pressure Regulator.....	42
II	Solenoid Valve and Pressure Transducer.....	42
III	Closely-Spaced Orifices Used to Produce Energy Loss..	43
IV	Recording and Calibrating Instrumentation.....	43
V	Water-Hammer Pressure-Time Diagram; Case 1(a) ; One Cycle.....	50
VI	Water-Hammer Pressure-Time Diagram; Case 1(a) ; Four Cycles.....	51
VII	Water-Hammer Pressure-Time Diagram; Case 1(b) ; One Cycle.....	52
VIII	Water-Hammer Pressure-Time Diagram; Case 1(b) ; Four Cycles.....	53
IX	Water-Hammer Pressure-Time Diagram; Case 1(c).....	54
X	Water-Hammer Pressure-Time Diagram; Case 1(d).....	55
XI	Water-Hammer Pressure-Time Diagram; Case 2(a).....	56
XII	Water-Hammer Pressure-Time Diagram; Case 2(b).....	57
XIII	Water-Hammer Pressure-Time Diagram; Case 2(c).....	58

NOMENCLATURE

Description	Units	Symbol Used	
		In Theory	In Computer Program
Wave Celerity	Ft/sec	a	A
Acceleration	Ft/sec ²	A _c	
Pipe wall thickness	Ft	b	B
Inside diameter of pipe	Ft	D	D
Modulus of elasticity	Lbs/ft ²	E	E
Pressure wave height	Ft	F, F ₁ , F ₂ , f ₁ , f ₂	
Friction factor		f	FR.
Acceleration of gravity	Ft/sec ²	g	
Piezometric head	Ft	H'	
Head at reservoir	Ft	H ₀	H ₀
Dimensionless piezometric head (H'/H ₀)		H	H or HP
Loss coefficient		K	KOR.
Bulk modulus of elasticity of water	Lbs/ft ²	K	K ₁
Total length of pipe	Ft	L	L
Reynolds Number		R	R
Time	Secs.	t'	
Dimensionless time (t'/(2L/A))		t	T
Time of valve closure	Secs.	t _c	TC
Velocity in pipe	Ft/sec	V'	
Steady-state velocity	Ft/sec	V ₀	V ₀
Dimensionless velocity (V'/V ₀)		V	V, VP

NOMENCLATURE

Description	Units	Symbol Used	
		In Theory	In Computer Program
Distance from reservoir	Ft	x'	
Dimensionless distance from reservoir (x/L)		x	X
Specific weight of water	Lbs/ft ³	γ	
Poisson's Ratio		μ	
Kinematic viscosity	Ft ² /sec	ν	NU
Mass density of water	Slugs/ft ³	ρ	
Ratio of effective gate opening to full gate opening		τ	TAU

I. HISTORICAL REVIEW

The first studies of water hammer date back to the beginning of the present century, when the contributions of Michaud⁽⁵⁶⁾, Joukowsky⁽³⁶⁾ and Allievi⁽¹⁾ pioneered the analytical treatment of this hydraulic problem. Joukowsky was the first to establish the rate of propagation of the wave, and prove that the head rise for instantaneous valve closure was equal to aV'/g , where a is the wave celerity, V' is the velocity in the pipe and g is the acceleration of gravity. Allievi developed the mathematical analysis of water hammer for uniform closures and presented charts for maximum pressure rise in simple conduits. Later authors extended Allievi's theory to consider changes of pipe diameter and pipe thickness, branch pipes, effects of air vessels and other complications. The solution to these different problems was obtained arithmetically by careful bookkeeping of the travel of the wave in the pipe system and the consequent changes in the head and the velocity of the water.

This step by step procedure of determining the pressure in a pipe system was slow and laborious and was readily given up in favor of a graphical procedure. The graphical solution of water-hammer problems was first suggested by Professor L. Bergeron⁽¹²⁾ and since then many authors^(4,6,7,8,72) have extended this method to many complicated problems ranging from pipelines with surge tanks and air vessels to transient conditions following shutoff of a pump feeding a long pipeline. These graphical procedures, however, were derived from equations which neglected friction effects and kinetic energy terms.

Whenever friction in a pipeline became an important factor, the graphical methods were modified to take this into account by concentrating the loss of the entire pipe length at one or more points in the pipeline. This approximation generally gave satisfactory results. Lately, however, interest in the solution of water-hammer problems has been revived because of the development of the method of characteristics^(26,53) for solving hyperbolic partial differential equations and the availability of high speed electronic computers to carry out the numerous calculations associated with the solution. These developments enable one to take into account those terms of the water-hammer equations which were hitherto neglected. The terms that were formerly deleted from the equations were the non-linear terms, including those resulting from the friction in the pipe or from the minor losses occurring at one or more points in the pipe. Thus, a more complete and accurate picture of the wave profile is made available by this procedure. The versatility and flexibility of this method also enables one to provide solutions to more complicated problems than could be handled previously.

II. INTRODUCTION

This thesis is concerned with the study of pressure-wave reflections produced when a water-hammer pressure wave encounters a device which produces an energy loss in the steady state. The device causing the energy loss may be a pipe bend, a tee joint, a valve that is open or partially closed or a restricting orifice. It is the intention of the author to determine the transmission and reflection coefficients of the water-hammer pressure wave and their relationship with the energy loss of the device.

The theoretical relationships are first determined by a simplified theory neglecting friction effects, i.e., by using the solution to the classical wave equations. They are then confirmed by the use of a more complete and accurate theory. In this theory, the partial differential equations for water-hammer, including friction effects, are solved by the method of characteristics and a high speed digital computer, the IBM 7090, is utilized for their numerical integration. From the output of the computer program, it is possible to calculate the values of the approaching, reflected and transmitted pressure waves, and knowing the magnitude of the minor loss, to verify their inter-relationships.

It is to be recognized at this point that this problem could be solved by the graphical methods of Schnyder-Bergeron.^(12,13) However, as with most graphical procedures, even though one can obtain the final solution one does not necessarily come to have a better understanding of the mechanics of the problem.

Finally, the results of an experimental verification of the theoretical relationships are set forth. The experiment consists of

producing a water-hammer pressure wave in a pipeline with an orifice in the middle and recording the pressure-time history at two points of the pipeline. This pressure-time diagram is superimposed on the theoretical diagram, obtained from the computer program, for the sake of comparison. Thus, the validity of the assumptions made in the derivation of the theory is affirmed.

III. ELEMENTARY SOLUTION

The theoretical study of water hammer reduces to the solution of two partial differential equations. As these equations have been derived in many texts (59,67,81) they will be used in this thesis directly. The first equation is derived from Newton's second law and is referred to as the condition of dynamic equilibrium.

$$\frac{\partial H'}{\partial x'} = \frac{-1}{g} \frac{\partial V'}{\partial t'} \quad (1)$$

where H' is the piezometric head in feet of water, t' is time in seconds and x' is distance in feet measured from the reservoir. The second equation is derived from considerations of continuity, in a horizontal pipe.

$$\frac{\partial H'}{\partial t'} = \frac{-a^2}{g} \frac{\partial V'}{\partial x'} \quad (2)$$

In Equation (2), a represents the wave velocity in the pipe and is obtained from the following formula.

$$a^2 = \frac{K/\rho}{1 + C_1 KD/Eb}$$

in which C_1 is a constant (29,59) depending on the way in which the ends of the pipe are restricted and on the Poisson ratio of the pipe wall material, and the other symbols are as defined on page (vii).

The simultaneous solution of these two equations is given by

$$H' - H_0 = F\left(t' + \frac{x'}{a}\right) + f\left(t' - \frac{x'}{a}\right) \quad (3)$$

where F and f are arbitrary functions of $\left(t' + \frac{x'}{a}\right)$ and $\left(t' - \frac{x'}{a}\right)$ respectively, and

$$V' - V_0 = \frac{-g}{a} \left\{ F\left(t' + \frac{x'}{a}\right) - f\left(t' - \frac{x'}{a}\right) \right\} \quad (4)$$

Thus the changes in head and velocity could be obtained if the functions F and f are known or these functions could be evaluated if the changes in head and velocity are known. Using these formulae, it is possible to calculate the reflections for certain boundary conditions, as shown below.

At a reservoir, $H' - H_0$ is zero at all times. Hence $f(t' - \frac{x'}{a}) = -F(t' + \frac{x'}{a})$ from Equation (3), and so $V' - V_0 = -\frac{2g}{a} F(t' + \frac{x'}{a})$.

At a Dead-End.

V' and V_0 are both zero at all times.

Hence, $f(t' - \frac{x'}{a}) = F(t' + \frac{x'}{a})$ from Equation (4).

Thus, $H' - H_0 = 2 F(t' + \frac{x'}{a})$.

Similarly, when a water-hammer pressure wave encounters a change in pipe area and/or wave speed, the reflected wave is equal to

$(A_1/a_1 - A_2/a_2)/(A_1/a_1 + A_2/a_2)$ times the approaching wave and the transmitted wave is equal to $(2A_1/a_1)/(A_1/a_1 + A_2/a_2)$ times the approaching wave.

The magnitudes of the reflected and the transmitted waves will now be derived when a water-hammer pressure wave encounters a minor loss.

Derivation

In Figure 1, let points A and B be on either side of the loss-producing device, in this case an orifice. Let F_1 be a water-hammer pressure wave approaching point A . Let f_1 be its reflection and F_2 its transmission. Let the head and velocity before F_1 reaches the orifice be H_{A0} , H_{B0} and V_{A0} , V_{B0} . Let the head and velocity after reflection and transmission be H_{At} , H_{Bt} , and V_{At} , V_{Bt} .

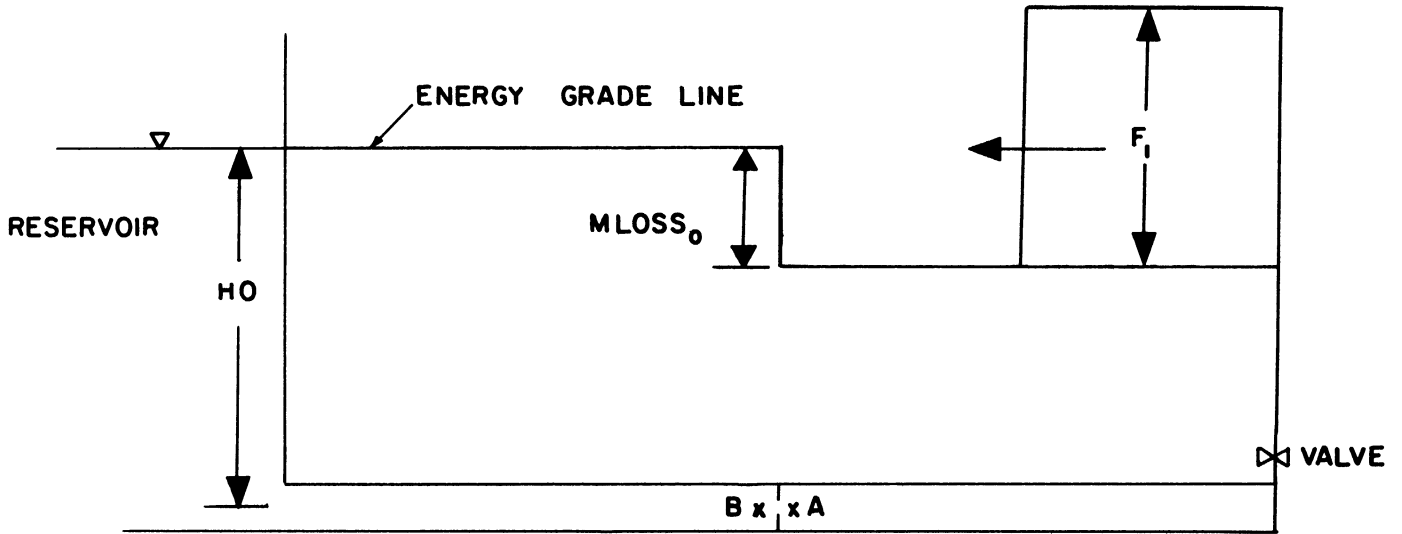


Figure 1(a). Conditions Before a Water-Hammer Pressure Wave Encounters a Minor Loss.

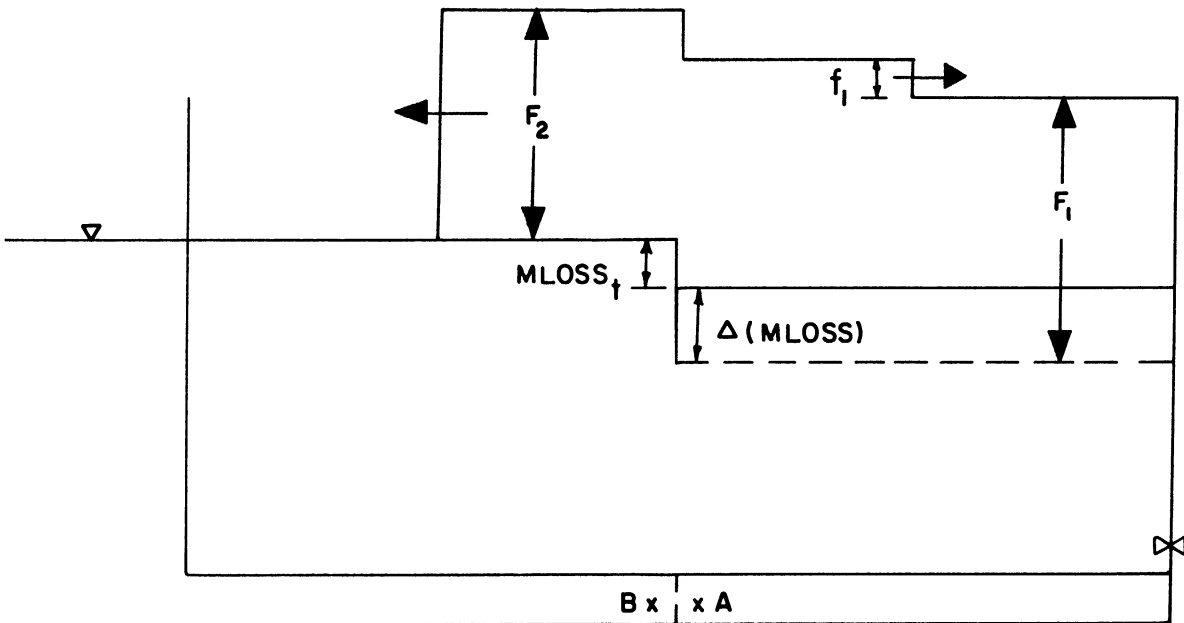


Figure 1(b). Conditions After a Water-Hammer Pressure Wave Encounters a Minor Loss.

14

From Equations (3) and (4),

$$H_{At} - H_{AO} = F_1 + f_1 \quad (5)$$

$$H_{Bt} - H_{BO} = F_2 \quad (6)$$

$$V_{At} - V_{AO} = -\frac{g}{a} (F_1 - f_1) \quad (7)$$

$$V_{Bt} - V_{BO} = -\frac{g}{a} F_2 \quad (8)$$

From the condition of continuity,

$$V_{At} = V_{Bt} \quad \text{and} \quad V_{AO} = V_{BO} \quad (9)$$

Hence, from (7), (8), and (9)

$$-\frac{g}{a} F_2 = -\frac{g}{a} (F_1 - f_1)$$

i.e. $F_2 = F_1 - f_1 \quad (10)$

Since a minor loss occurs at the orifice,

$$H_{BO} - H_{AO} = \text{MLOSS}_O \quad \text{and} \quad H_{Bt} - H_{At} = \text{MLOSS}_t \quad (11)$$

From (5), (6), and (11),

$$F_2 - F_1 - f_1 = \text{MLOSS}_t - \text{MLOSS}_O = \Delta(\text{MLOSS}) \quad (12)$$

From (10), and (12), we have

$$-2f_1 = \Delta(\text{MLOSS})$$

Therefore,

$$f_1 = - \frac{\Delta(\text{MLOSS})}{2} \quad (13)$$

and from (10),

$$F_2 = F_1 + \frac{\Delta(\text{MLOSS})}{2} \quad (14)$$

Thus, it can be seen that the reflection is dependent only upon the change in the minor loss before and after the passage of the wave. The transmitted wave is equal to the approaching wave plus half the change in the minor loss.

The change in the minor loss is easily evaluated when the velocity behind the approaching wave F_1 is zero or very nearly zero. This is so when instantaneous closure of the valve occurs, and the pipeline is considered frictionless. For this case,

$$\Delta(\text{MLOSS}) = - K \frac{V_{AO}^2}{2g} \quad (15)$$

Hence,

$$f_1 = \frac{1}{2} K \frac{V_{AO}^2}{2g} \quad (16)$$

and

$$F_2 = F_1 - \frac{1}{2} K \frac{V_{AO}^2}{2g} \quad (17)$$

However, when the velocity behind the wave F_1 is not zero, Equations (16) and (17) do not apply and f_1 becomes a more complicated function of F_1 . This relationship is found in the following manner.

Let

$$\text{MLOSS} = K \frac{V_{AO}^2}{2g} = K \frac{V_{BO}^2}{2g} \quad \text{and} \quad \text{MLOSS}_t = K \frac{V_{At}^2}{2g} = K \frac{V_{Bt}^2}{2g}$$

Therefore,

$$\Delta(\text{MLOSS}) = \frac{K}{2g} (V_{At}^2 - V_{AO}^2)$$

From Equation (7),

$$\begin{aligned} V_{At} - V_{AO} &= \frac{-g}{a} \{F_1 - f_1\} = \frac{-g}{a} \left\{F_1 + \frac{\Delta(MLOSS)}{2}\right\} \\ &= \frac{-g}{a} \left\{F_1 + \frac{K}{4g} (V_{At}^2 - V_{AO}^2)\right\} \end{aligned}$$

$$\text{Let } \Delta V_A = V_{At} - V_{AO}$$

$$\begin{aligned} \text{Then } \Delta V_A &= \frac{-g}{a} F_1 - \frac{K}{4a} (V_{At} - V_{AO})(V_{At} + V_{AO}) \\ &= \frac{-g}{a} F_1 - \frac{K}{4a} \Delta V_A (\Delta V_A + 2V_{AO}) \\ &= \frac{-g}{a} F_1 - \frac{K(\Delta V_A)^2}{4a} - \frac{KV_{AO}}{2a} \Delta V_A \end{aligned}$$

or

$$\frac{K}{4a} (\Delta V_A)^2 + \Delta V_A \left(1 + \frac{K}{2a} V_{AO}\right) + \frac{gF_1}{a} = 0$$

Therefore

$$\begin{aligned} \Delta V_A &= \frac{2a}{K} \left\{ -\left(1 + \frac{KV_{AO}}{2a}\right) \pm \sqrt{\left(1 + \frac{KV_{AO}}{2a}\right)^2 - 4 \frac{K}{4a} \frac{gF_1}{a}} \right\} \\ &= -\left(\frac{2a}{K} + V_{AO}\right) \pm \sqrt{\left(\frac{2a}{K} + V_{AO}\right)^2 - \frac{KgF_1}{a^2} \frac{4a^2}{K^2}} \\ &= -\left(\frac{2a}{K} + V_{AO}\right) \pm \sqrt{\left(\frac{2a}{K} + V_{AO}\right)^2 - \frac{4gF_1}{K}} \end{aligned}$$

But

$$\Delta V_A = -\frac{g}{a} (F_1 - f_1)$$

Therefore

$$-\frac{g}{a} (F_1 - f_1) = -\left(\frac{2a}{K} + V_{AO}\right) \pm \sqrt{\left(\frac{2a}{K} + V_{AO}\right)^2 - \frac{4gF_1}{K}}$$

Therefore

$$f_1 = F_1 - \frac{a}{g} \left(\frac{2a}{K} + V_{AO}\right) \pm \frac{a}{g} \sqrt{\left(\frac{2a}{K} + V_{AO}\right)^2 - \frac{4gF_1}{K}} \quad (18)$$

and

$$F_2 = \frac{a}{g} \left(\frac{2a}{K} + V_{AO}\right) \mp \frac{a}{g} \sqrt{\left(\frac{2a}{K} + V_{AO}\right)^2 - \frac{4gF_1}{K}} \quad (19)$$

It is easy to prove that in Equation (18), the positive sign before the radical is the correct one. In the limiting case, when $V_{At} = 0$, Equation (18) should reduce down to Equation (16).

$$\text{When } V_{At} = 0, \quad F_1 = \frac{a V_{AO}}{g}$$

From (18)

$$\begin{aligned} f_1 &= \frac{aV_{AO}}{g} - \frac{2a^2}{gK} - \frac{aV_{AO}}{g} \pm \frac{a}{g} \sqrt{\left(\frac{2a}{K} + V_{AO}\right)^2 - \frac{4g}{K} \frac{aV_{AO}}{g}} \\ &= -\frac{2a^2}{gK} \pm \frac{a}{g} \sqrt{\frac{4a^2}{K^2} + V_{AO}^2 + \frac{4aV_{AO}}{K} - \frac{4aV_{AO}}{K}} \end{aligned}$$

Expanding $\left(\frac{4a^2}{K^2} + V_{AO}^2\right)^{1/2}$ by the Binomial Theorem,

$$\begin{aligned} f_1 &= -\frac{2a^2}{gK} \pm \frac{a}{g} \left\{ \left(\frac{4a^2}{K^2}\right)^{1/2} + \frac{1}{2} \left(\frac{4a^2}{K^2}\right)^{-1/2} V_{AO}^2 - \frac{1}{16} \left(\frac{4a^2}{K^2}\right)^{-2} V_{AO}^4 + \dots \right\} \\ &= -\frac{2a^2}{gK} \pm \frac{2a^2}{gK} \pm \frac{1}{2} K \frac{V_{AO}^2}{2g} \mp \frac{K^3 V_{AO}^2}{128a^3} K \frac{V_{AO}^2}{2g} + \dots \\ &= \pm \frac{1}{2} K \frac{V_{AO}^2}{2g}, \text{ neglecting terms of smaller magnitude. Thus,} \end{aligned}$$

the positive sign is correct in Equation (18) and hence the negative sign is the correct one in Equation (19).

The series expansion of $\left(\frac{4a^2}{K^2} + V_{AO}^2\right)^{1/2}$ by the Binomial Theorem is convergent whenever $\frac{KV_{AO}^2}{2g} \leq \frac{aV_{AO}}{g}$. This condition is always fulfilled as the minor loss in a pipeline is generally much smaller than the water-hammer pressure wave height.

The procedure is the same when analyzing the situation in which an f_1 wave approaches a minor loss, as in the case of flow establishment in a pipe. It can be shown that the reflected wave $F_1 = -\frac{\Delta(\text{MLOSS})}{2}$ and that the transmitted wave is equal to $(f_1 + \frac{\Delta(\text{MLOSS})}{2})$.

More complicated situations could also be handled in the same manner. For example, consider the situation in which an F_1 wave approaches a minor loss from the right-hand side and an F_2 wave approaches it from the left-hand side and both the waves encounter the minor loss at the same time. It can be shown that the reflected wave on the right-hand side, $f_1 = f_2 - \frac{\Delta(\text{MLOSS})}{2}$ and that the reflected wave on the left-hand side is equal to $F_1 + \frac{\Delta(\text{MLOSS})}{2}$.

IV. SOLUTION BY THE METHOD OF CHARACTERISTICS

The basic partial differential equations for water hammer in a pipe, taking into account friction effects, have been derived in Reference 78, and will be used directly in this thesis.

The assumptions made in the derivation are listed below.

1. Uniform velocity and pressure distribution over area of pipe.
2. Pipe wall material and liquid in pipe are perfectly elastic and homogeneous.
3. The pipe remains full of liquid at all points and at all times.
4. The static pressure in pipe is above the vapor pressure of liquid at all times.
5. The elastic hysteresis of liquid is assumed negligible.

The equations will be non-dimensionalized and their characteristic equations derived. The purpose of non-dimensionalizing is so that the same notation may be used here as is used in the conjugate equations of the graphical procedure. It will be seen later that these conjugate equations are a particular case of the characteristic equations derived here. These characteristic equations are then transformed into their finite-difference form and used for the solution of the head and velocity in the computer program. Next, the equations at the following boundary conditions are derived; at the reservoir end, at the valve end, both for time less than valve-closure time and for time after valve closure. Finally, the boundary conditions at a minor loss are derived in finite-difference form.

Derivation of Characteristic Equations

The following two partial differential equations are the ones whose simultaneous solution gives the head and velocity (the dependent variables) in terms of the distance and time (the independent variables). These equations are quasi-linear and of the hyperbolic type. They include a term which takes into account the friction loss in the pipe, and those terms which were neglected in the classical water-hammer theory have been retained.

The condition of equilibrium,

$$\frac{\partial H'}{\partial x'} + \frac{f}{D} \frac{(V')^2}{2g} = - \frac{1}{g} \left(\frac{\partial V'}{\partial t'} + V' \frac{\partial V'}{\partial x'} \right) . \quad (20)$$

The condition of continuity, for horizontal pipes,

$$\frac{\partial H'}{\partial t'} + V' \frac{\partial H'}{\partial x'} = - \frac{a^2}{g} \frac{\partial V'}{\partial x'} \quad (21)$$

In order to non-dimensionalize these equations, let

$$\frac{H'}{H_0} = H, \quad \frac{V'}{V_0} = V, \quad \frac{x'}{L} = x \quad \text{and} \quad \frac{t'}{2L/a} = t .$$

Also let $\frac{\partial H}{\partial x} = H_x, \quad \frac{\partial H}{\partial t} = H_t, \quad \frac{\partial V}{\partial x} = V_x \quad \text{and} \quad \frac{\partial V}{\partial t} = V_t .$

This transforms Equations (20) and (21) into

$$\frac{H_0}{L} H_x + \frac{fV_0^2}{2gD} V^2 = - \frac{1}{g} \left\{ \frac{aV_0}{2L} V_t + \frac{V_0^2}{L} V V_x \right\} \quad (22)$$

and

$$\frac{aH_0}{2L} H_t + \frac{V_0H_0}{L} V H_x = - \frac{a^2}{g} \frac{V_0}{L} V_x \quad (23)$$

To determine the characteristic equations, let

$$J_1 = \frac{HO}{L} H_x + \frac{f VO^2}{2gD} V^2 + \frac{VO}{gL} \left\{ \frac{a}{2} V_t + VO V V_x \right\} = 0$$

and

$$J_2 = \frac{aHO}{2} H_t + VO HO V H_x + \frac{a^2}{g} VO V_x = 0$$

Multiplying J_1 by $2gL/aVO$ and J_2 by $2/aHO$ and putting $\beta = aVO/2gHO$; we have,

$$J'_1 = H_x/\beta + \frac{fLVO}{aD} V^2 + V_t + \frac{2 VO V}{a} V_x = 0$$

$$J'_2 = H_t + \frac{2 VO}{a} V H_x + 4\beta V_x = 0$$

Combining J'_1 and J'_2 linearly with an undetermined multiplier λ ,

$$J = J'_1 + \lambda J'_2 = \frac{1}{\beta} H_x + \frac{fLVO}{aD} V^2 + V_t + \frac{2 VO}{a} V V_x + \lambda \left\{ H_t + \frac{2 VO}{a} V H_x + 4\beta V_x \right\} = 0$$

Rearranging the terms, we have

$$\left\{ \frac{1}{\beta} + \lambda \frac{2 VO V}{a} \right\} H_x + \lambda H_t + \left\{ \frac{2 VO}{a} V + \lambda 4 \beta \right\} V_x + V_t + \frac{fLVO}{aD} V^2 = 0 \quad (24)$$

Now, since V and H are both functions of x and t ,

$$dH = H_x dx + H_t dt$$

and

$$dV = V_x dx + V_t dt$$

or

$$\frac{dH}{dt} = H_x \frac{dx}{dt} + H_t$$

and

$$\frac{dV}{dt} = V_x \frac{dx}{dt} + V_t$$

With the last two equations in mind, Equation (24) could be reduced to the following simple form,

$$\lambda \frac{dH}{dt} + \frac{dV}{dt} + \frac{f L V_0}{a D} V^2 = 0 \quad (25)$$

if at the same time we make,

$$\frac{dx}{dt} = \frac{1}{\lambda} \left\{ \frac{1}{\beta} + \lambda \frac{2 V_0 V}{a} \right\} \quad (26)$$

and

$$\frac{dx}{dt} = \left\{ \frac{2 V_0 V}{a} + \lambda 4 \beta \right\} \quad (27)$$

From Equations (26) and (27),

$$\frac{1}{\lambda} \left\{ \frac{1}{\beta} + \lambda \frac{2 V_0 V}{a} \right\} = \frac{2 V_0 V}{a} + \lambda 4 \beta$$

Therefore,

$$\lambda^2 = \frac{1}{4\beta^2}$$

or,

$$\lambda = \pm \frac{1}{2\beta} \quad (28)$$

Substituting back in Equation (27),

$$\frac{dx}{dt} = \frac{2 V_0 V}{a} \pm 2 \quad (29)$$

Since the term $\frac{2 V_0 V}{a}$ is small compared with the other term, we can approximate Equation (29) by

$$\frac{dx}{dt} = \pm 2 \quad (30)$$

and the characteristic equations for V and H become,

$$dt J = dV + \frac{1}{2\beta} dH + \frac{f L V_0}{a D} V^2 dt = 0 \quad (31)$$

and

$$dt J = dV - \frac{1}{2\beta} dH + \frac{f L V_0}{a D} V^2 dt = 0 \quad (32)$$

Summing up, the simultaneous solution of the partial differential Equations (22) and (23) has been reduced to the solution of two total differential Equations (31) and (32), in the two directions given by Equations (30). The solution is thus seen to involve two planes, the (x,t) plane and the (V,H) plane. The lines in the (x,t) plane are straight lines as shown by Equations (30), whilst those in the (V,H) plane are curved because of the V^2 term in Equations (31) and (32). These lines are called characteristics and will be referred to as the C_+ and C_- characteristics. See Figure 2.

Thus, along the C_+ characteristic,

$$dx - 2 dt = 0 \quad (33)$$

and

$$dV + \frac{1}{2\beta} dH + \frac{f L V_0}{a D} V^2 dt = 0 \quad (34)$$

And, along the C_- characteristic,

$$dx + 2 dt = 0 \quad (35)$$

and

$$dV - \frac{1}{2\beta} dH + \frac{f L V_0}{a D} V^2 dt = 0 \quad (36)$$

From Equations (34) and (36), it can be seen that, when the friction term is neglected, the characteristic equations become

$$dV = \pm \frac{1}{2\beta} dH$$

The above equations are precisely the conjugate equations used in the graphical analysis of water hammer and can be seen to be a particular case of the more general solution provided here.

Finite-Difference Equations

Since the general solution to hyperbolic, partial differential equations is yet unknown, particular solutions for individual cases under study are usually sought.

A close examination of Equations (33) to (36) reveals that all the terms, except the friction terms, are exact differentials and hence can be integrated easily and without any error. Integration of the friction terms along their respective characteristics between two points 0 and 1 yields

$$\frac{L V_0}{a D} \int_0^1 (f V^2) dt .$$

This integral can be approximated in finite-difference form in several ways. The first-order approximation assumes the function to have a constant value during the interval dt .

Hence,

$$\frac{L V_0}{a D} \int_0^1 (f V^2) dt = \frac{L V_0}{a D} (f V^2)_0 (t_1 - t_0) \quad (37)$$

The second order approximation makes use of the trapezoidal rule to estimate the value of the integral.

Hence,

$$\frac{L V_0}{aD} \int_0^1 (f v^2) dt = \frac{L V_0}{aD} \frac{1}{2} \{ (f v^2)_0 + (f v^2)_1 \} (t_1 - t_0) \quad (38)$$

The error involved in Equation (38) is smaller than that in Equation (37). However, certain extrapolation procedures⁽⁵³⁾ are known whereby Equation (37) could be used and the error kept to the same order of magnitude as that of Equation (38). It will be shown later why Equation (37) was used in preference to Equation (38).

Equations (33) to (36) will now be integrated along their respective characteristics from a point 0 at which V and H are known to another point 1 at which V and H are unknown. Thus, along C₊,

$$(x_1 - x_0) - 2(t_1 - t_0) = 0 \quad (39)$$

and

$$(V_1 - V_0) + (H_1 - H_0)/2\beta + \frac{L V_0}{aD} (f v^2)_0 (t_1 - t_0) = 0 \quad (40)$$

Along C₋,

$$(x_1 - x_0) + 2(t_1 - t_0) = 0 \quad (41)$$

and

$$(V_1 - V_0) - (H_1 - H_0)/2\beta + \frac{L V_0}{aD} (f v^2)_0 (t_1 - t_0) = 0 \quad (42)$$

The Equations (39) to (42) will now be used to obtain solutions to the head and velocity at specified points along a uniform pipe and at regular intervals of time. This procedure is known as the

Specified Time Interval Method. As illustrated in Figure 3 on page 21, the pipe is divided into N number of sections. The time interval used is then $\frac{1}{2N}$. From the initial, steady-state conditions in the pipe, the values of V and H at each point of the pipe will be known. From these values, it will be possible to calculate V and H for $t = \Delta t$ at the points marked with a black dot in Figure 3. From the known end conditions, it will be possible to determine V and H at the points marked with a cross for $t = \Delta t$. This procedure is then repeated for $t = 2 \Delta t$ and so on, for any time length.

Finite-Difference Equations for a Uniform Pipe

Let the head and velocity at time $t = t_{j-1}$ be known for all intervals of x. See Figure 4. Suppose the solution at $P(x_i, t_j)$ is to be sought. Let the two characteristics through P, with Equations (39) and (41), cut the line $t = t_{j-1}$ at R and S. By means of interpolation, the head and velocity at R and S could be determined from the values at A, B and C. Then from Equations (40) and (42) we have,

$$(V_P - V_R) + (H_P - H_R)/2\beta + \frac{L V_0}{aD} (f V^2)_R (t_P - t_R) = 0 \quad (43)$$

and

$$(V_P - V_S) - (H_P - H_S)/2\beta + \frac{L V_0}{aD} (f V^2)_S (t_P - t_S) = 0 \quad (44)$$

Making $(t_P - t_R) = (t_P - t_S) = \Delta t$, and solving the above two equations for V_P and H_P , we have,

$$V_P = \frac{V_R + V_S}{2} - (H_S - H_R)/4\beta - \frac{L V_0 \Delta t}{2 aD} \{(f V^2)_R + (f V^2)_S\} \quad (45)$$

$$H_P = \frac{H_R + H_S}{2} - \beta(V_S - V_R) + \beta \frac{L V_0 \Delta t}{aD} \{(f V^2)_S - (f V^2)_R\} \quad (46)$$

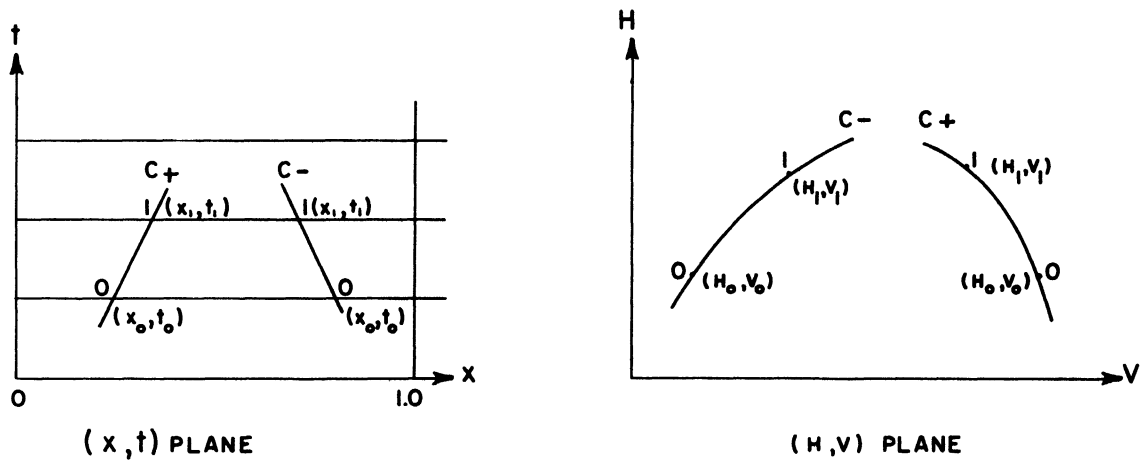


Figure 2. Characteristics.

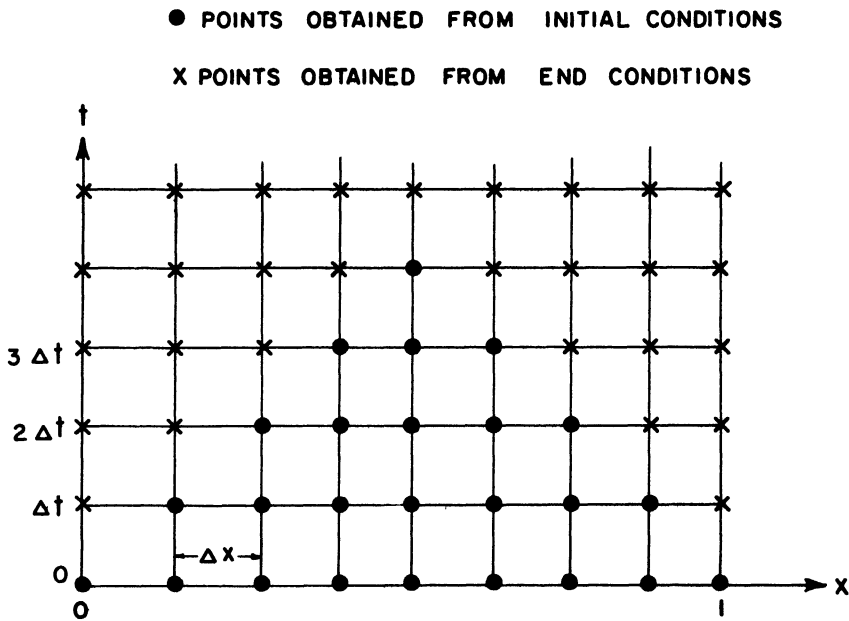


Figure 3. Specified Time-Interval Method.

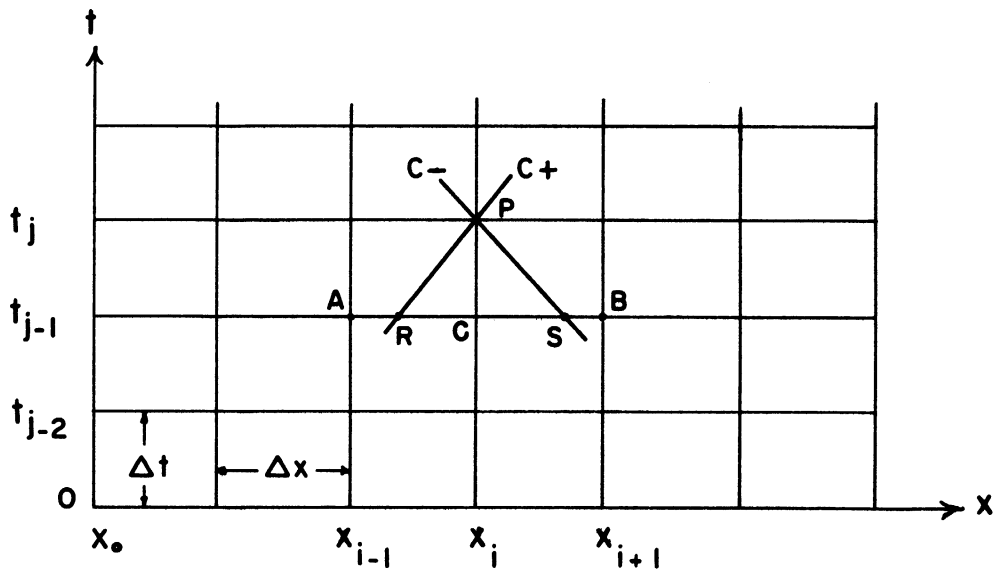


Figure 4. The (x,t) Plane for a Uniform Pipe.

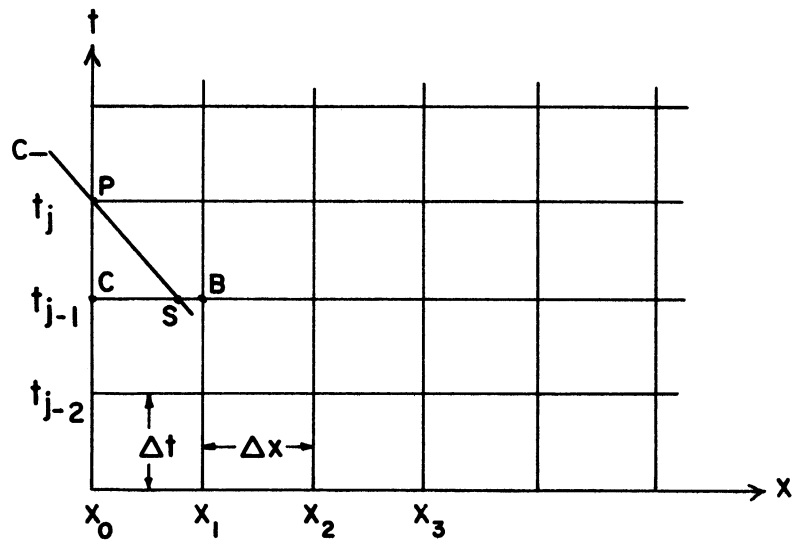


Figure 5. The (x,t) Plane for a Left-Hand Boundary Condition.

Whenever Δt is chosen to be exactly $\Delta x/2$, then the points R and S coincide with A and B respectively. This value of Δt then makes the interpolation procedure unnecessary and leads to a speedier solution.

At this stage, it can be seen why Equation (37) is easier to use than Equation (38). If Equation (38) was used, the solution for V_p and H_p for a uniform pipe would be as follows.

$$V_P = \frac{V_R + V_S}{2} - (H_S - H_R)/4\beta - \frac{L V_0 \Delta t}{4 aD} \{(f V^2)_R + (f V^2)_S + 2(f V^2)_P\}$$

$$H_P = \frac{H_R + H_S}{2} - (V_S - V_R) \beta + \frac{\beta L V_0 \Delta t}{2 aD} \{(f V^2)_S - (f V^2)_R\}$$

It is clear that the first equation cannot be solved explicitly for V_p , as the friction factor f is a function of V_p . Thus, the solution would have to be carried out by an iterative procedure by assuming an initial value of V_p . Because of this and also since Δt was very small, it was decided that Equation (37) provided sufficient accuracy.

Boundary Conditions:

a. A Reservoir at the Left-Hand End.

Consider Figure 5 on page 22. Let a constant head reservoir exist at x_0 . Hence, at all times,

$$H_p = 1.0 \tag{47}$$

Let the C_- characteristic through P cut $t = t_{j-1}$ in S, then from Equation (42)

$$(V_P - V_S) - (1.0 - H_S)/2\beta + \frac{L V_0}{aD} (f V^2)_S \Delta t = 0$$

or

$$V_P = V_S + (1.0 - H_S)/2\beta - \frac{L V_0}{aD} (f V^2)_S \Delta t \tag{47A}$$

b. A Valve at the Right Hand End.

(i) For Time t Less Than Valve-Closure Time t_c .

Whenever $t < t_c$, the head and velocity at the valve have to be determined from two conditions. The first is the water-hammer equation, $\Delta H = -2\beta \Delta V$ and the second is the orifice equation $Q = C_d \cdot A_{\text{valve}} \sqrt{2gH'_V}$, where H'_V is the head loss across the valve. The orifice equation is usually rewritten in the following form.

$$V = \tau \sqrt{H'_V}$$

where

$$\tau = \frac{(C_d A_{\text{valve}})_{t=t}}{(C_d A_{\text{valve}})_{t=0}}$$

The values of τ are determined experimentally as a function of time t . Using the appropriate value of τ , solution of the two equations gives V and H at the valve.

However, in this thesis, the conditions at a valve are treated differently. In the experimental set-up, the solenoid valve does not discharge into the atmosphere. Instead, the pipeline continues after the valve and hence the pressure downstream from the valve has also to be found. For this reason, the valve was treated as a device causing a sharp energy loss at a point in the pipeline. The equations for this condition are derived a little later in the thesis.

The τ values obtained experimentally are transformed into values of loss coefficients in the following manner.

$$V = \tau \sqrt{H'_V}$$

or

$$\begin{aligned} H'_V &= \frac{2g}{\tau^2} \frac{V^2}{2g} \\ &= K_{SV} \frac{V^2}{2g} \end{aligned}$$

Therefore

$$K_{SV} = \frac{2g}{\tau^2}$$

These values of loss coefficients are used in the equations derived later.

(ii) For Time t Greater Than Valve-Closure Time t_c .

Refer to Figure 6 on page 26 . When the valve is closed, the velocity at $x = l$ is always zero. Let the C_+ characteristic through P cut $t = t_{j-1}$ in R.

Then

$$(V_P - V_R) + (H_P - H_R)/2\beta + \frac{L}{aD} \frac{V_0}{V} (f V^2)_R \Delta t = 0$$

But

$$V_P = 0 \tag{48}$$

Hence,

$$H_P = H_R + 2\beta V_R - 2\beta \frac{L}{aD} \frac{V_0}{V} (f V^2)_R \Delta t \tag{49}$$

c. At a Minor Loss In the Pipe Line.

Refer to Figure 7 on page 26. Let a minor loss of $\frac{KV^2}{2g}$ take place at x_i and let P_1 and P_2 be points just upstream and just downstream of x_i respectively. Let the C_+ characteristic through P_1 cut the line $t = t_{j-1}$ in R and the C_- characteristic through P_2 cut $t = t_{j-1}$ in S. The four unknowns to be determined are V_{P1} , V_{P2} , H_{P1} and H_{P2} . The four available equations to determine them are the two characteristic equations, the continuity equation and equation of motion at $t = t_i$.

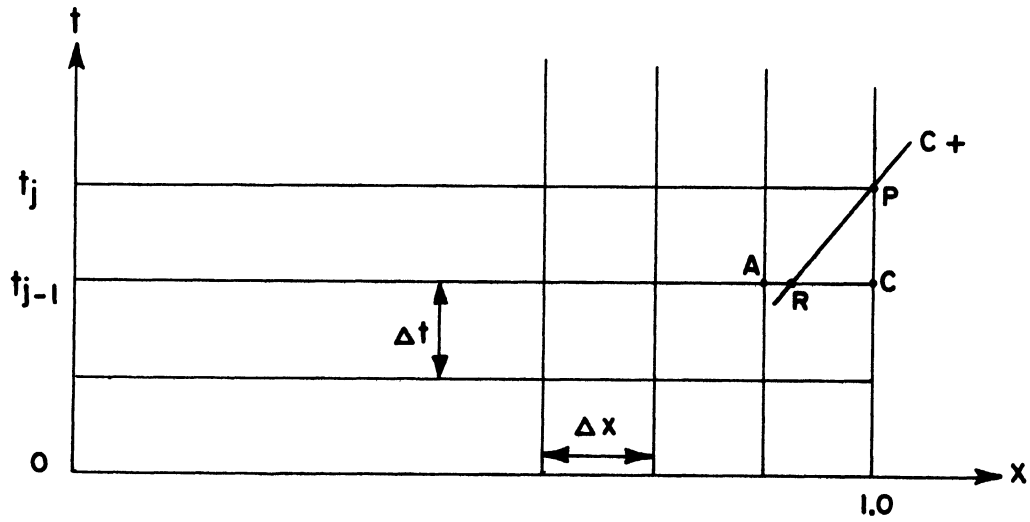


Figure 6. The (x,t) Plane for Right-Hand Boundary Condition.

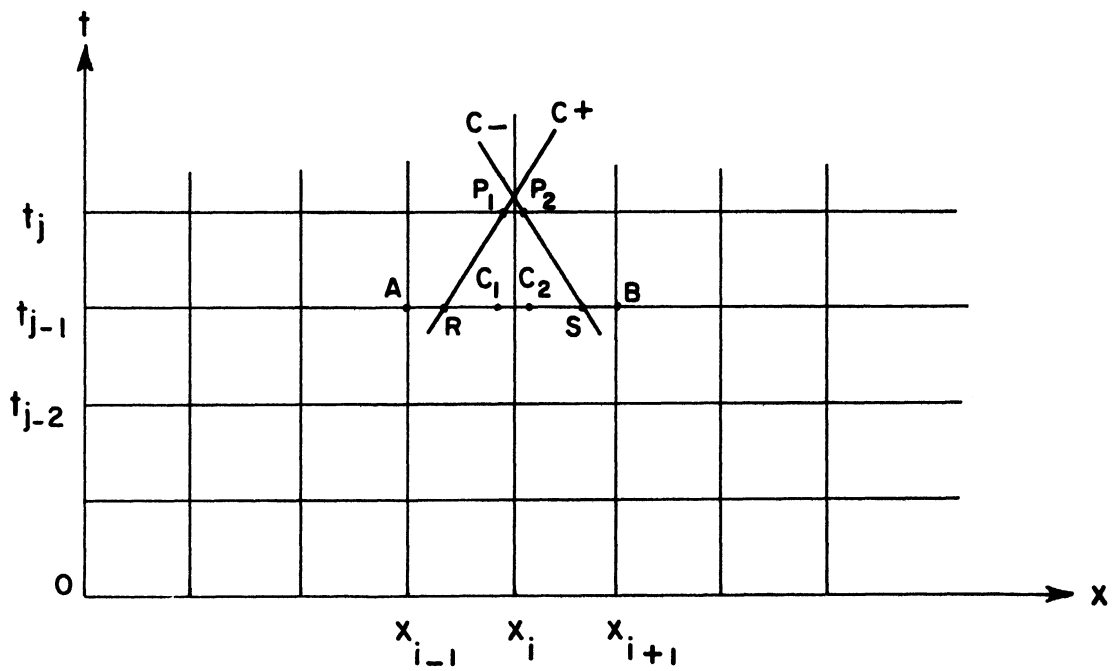


Figure 7. The (x,t) Plane for a Minor Loss Boundary Condition.

From Equation (40),

$$(V_{P1} - V_R) + (H_{P1} - H_R)/2\beta + \frac{L V_0}{aD} (f V^2)_R \Delta t = 0 \quad (50)$$

From Equation (42),

$$(V_{P2} - V_S) - (H_{P2} - H_S)/2\beta + \frac{L V_0}{aD} (f V^2)_S \Delta t = 0 \quad (51)$$

If the pipe diameter remains unchanged, continuity makes

$$V_{P1} = V_{P2} \quad (52)$$

The fourth equation is the equation of motion between the points P_1 and P_2 at time $t = t_i$. The unsteady equation of motion for an incompressible, inviscid fluid in dimensional form is

$$\begin{aligned} \frac{(V'_{P1})^2}{2} + gH'_{P1} + gZ'_{P1} + \int_0^{x'_{P1}} \frac{\partial(V'_{P1})}{\partial t'} dx' \\ = \frac{(V'_{P2})^2}{2} + gH'_{P2} + gZ'_{P2} + \int_0^{x'_{P2}} \frac{\partial(V'_{P2})}{\partial t'} dx' \end{aligned} \quad (53)$$

Now, $V'_{P1} = V'_{P2}$ and if the pipe is horizontal, $z'_{P1} = z'_{P2}$, and Equation (53) reduces to

$$gH'_{P1} = gH'_{P2} + \int_{x'_{P1}}^{x'_{P2}} \frac{\partial V'}{\partial t'} dx' \quad (54)$$

Since the two points P_1 and P_2 can be chosen arbitrarily close, the last term can be made as small as to make it negligible. Also, since a minor loss takes place between P_1 and P_2 , Equation (54) can be modified to take this into account.

Thus,

$$gH'_{P1} = gH'_{P2} + K(V'_{P1})^2/2$$

Or,

$$H'_{P1} = H'_{P2} + K(V'_{P1})^2/2g$$

Non-dimensionalizing the above equation, we have

$$H_{P1} = H_{P2} + \frac{K}{2g} \frac{V_0^2}{H_0} (V_{P1})^2 \quad (55)$$

Solving Equations (50), (51), (52) and (55) simultaneously, we get

$$H_{P1} = (H_R + H_S)/2 - \beta(V_S - V_R) + \beta \frac{L}{aD} \frac{V_0 \Delta t}{aD} \{(f v^2)_S - (f v^2)_R\} + \frac{1}{2} \frac{K}{2g} \frac{V_0^2}{H_0} V_{P1}^2 \quad (56)$$

$$H_{P2} = (H_R + H_S)/2 - \beta(V_S - V_R) + \beta \frac{L}{aD} \frac{V_0 \Delta t}{aD} \{(f v^2)_S - (f v^2)_R\} - \frac{1}{2} \frac{K}{2g} \frac{V_0^2}{H_0} V_{P1}^2 \quad (57)$$

$$V_{P1} = V_{P2} = (V_R + V_S)/2 + (H_R - H_S)/4\beta - \frac{L}{2} \frac{V_0 \Delta t}{aD} \{(f v^2)_R + (f v^2)_S\} - \frac{1}{2\beta} \cdot \frac{1}{2} \frac{K}{2g} \frac{V_0^2}{H_0} V_{P1}^2 \quad (58)$$

Equation (58) is a quadratic and hence can be solved explicitly for V_{P1} . This value of V_{P1} can then be used in Equations (56) and (57) to obtain the head before and after the minor loss. It should be recognized that these equations have been derived for positive velocities and hence when the velocities are negative, the friction and minor loss terms change sign. This is taken into account by replacing each v^2 term by $V|V|$, which automatically changes the sign.

A comparison between the equation for H_{p1} and the equation for head in a uniform pipe [Equation (46)] shows that the difference between them is half the minor loss. This conclusion was also arrived at from the classical wave theory [Equation (13)].

In the use of Equations (56), (57) and (58), it should be determined, whether the loss coefficient should have the steady-state value K or whether an unsteady loss-coefficient K_u should be used. Experiments^(18,19) have shown that for accelerated flow, K_u is less than K and that K_u decreases with increasing acceleration. The value of K_u is shown to be a function of the acceleration parameter $A_c L / (V')^2$.

Thus,

$$K_u = K - C_1 A_c L / (V')^2 \quad (59)$$

where C_1 is a constant of proportionality dependent upon the ratio of orifice area to pipe area.

This thesis, however, made use only of the steady state loss coefficient K because of the following reasons. First, experimental values of C_1 were not available for the low ratio of orifice to pipe area used in the experiment. Second, formula (59) would not be valid for the very high accelerations the fluid encounters upon passage of a water-hammer wave. For the case of instantaneous or rapid gate closure, the acceleration of the fluid approaches infinity each time a water-hammer wave passes by. This would imply from Equation (59) that K_u would become zero or even negative. For these reasons, it was decided that the steady-state loss coefficient should be used.

d. At a Valve Discharging Into the Atmosphere.

This condition is a particular case of the conditions at a minor loss described in the last section. The pressure at P_2 (refer Figure 8) is always atmospheric, i.e., $H_{P2} = 0$. Hence, there are only three unknowns to be determined. They are H_{P1} , V_{P1} and V_{P2} . The following are the three equations to be used for their solution.

From the C_+ characteristic [Equation (40)]

$$(V_{P1} - V_R) + (H_{P1} - H_R)/(2\beta) + L V_0 (f V^2)_R (t_P - t_R)/(a D) = 0 \quad (60)$$

From the condition of continuity,

$$V_{P1} = V_{P2} \quad (61)$$

The minor loss equation gives

$$\begin{aligned} H_{P1} &= H_{P2} + K V_0^2 V_{P1}^2 / (2g H_0) \\ &= K V_0^2 V_{P1}^2 / (2g H_0) \end{aligned} \quad (62)$$

Solving Equations (60), (61) and (62) simultaneously, we obtain

$$\frac{K V_0^2}{2g H_0} (V_{P1})^2 + 2\beta V_{P1} - H_R - 2\beta V_R - 2\beta \frac{L V_0 \Delta t}{a D} (f V^2)_R = 0 \quad (63)$$

Equation (63) is a quadratic in V_{P1} and hence its value could be easily obtained. Substituting its value in Equation (62) gives H_{P1} directly.

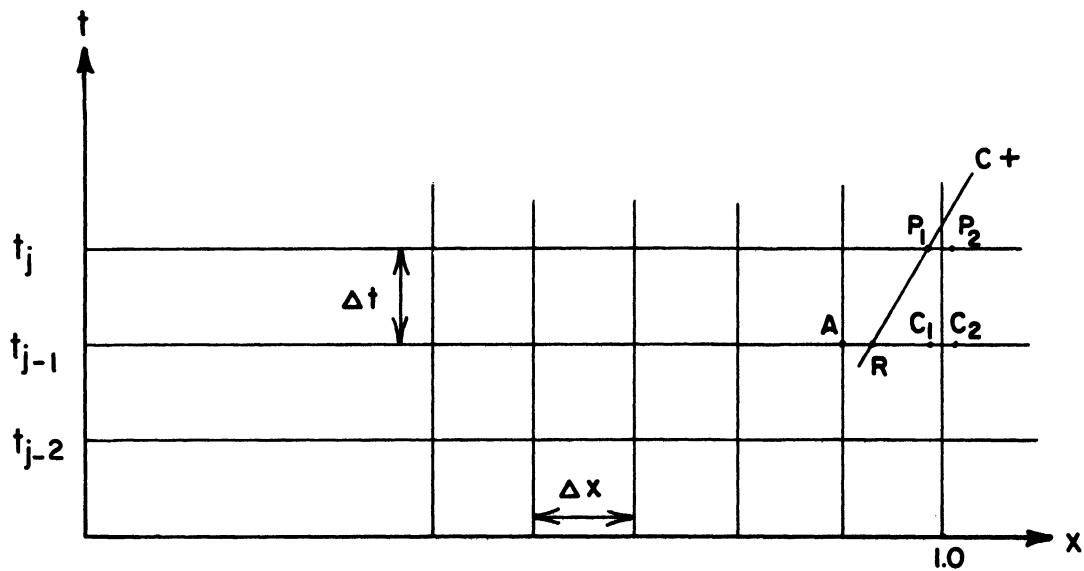


Figure 8. The (x,t) Plane for a Valve as a Right-Hand Boundary Condition.

V. EXPERIMENTAL SET-UP

The experimental set-up was organized in such a way that the reflection from a minor loss could be seen and compared with the minor loss. In order to make the reflection large, the minor loss also had to be made as large as possible. This was achieved by selecting a device with a very large loss coefficient. This device was placed in the middle of the pipeline and the pressure in the pipeline at two different points was recorded and compared with the theoretical results.

A schematic diagram of the experimental set-up is shown in Figure 9. At one end of the pipeline is a compression chamber, half filled with water and with compressed air in the space above the water level. The pressure of the air in the compression chamber is maintained at a constant level by means of a pressure regulator placed between the chamber and the compressor. In this way, the air pressure stayed constant even when the level of the water in the chamber dropped during the course of the experiment.

Twenty feet from the pressure chamber, three closely-spaced orifices were placed in the pipeline to produce a large energy loss (Figure 10, page 34). Steady state experiments were conducted to determine the loss coefficient of this device as a function of the Reynolds number. The results of the steady state experiments are shown in Figure 11.

The pipeline used was a hard copper tube, $1/2$ inch inside diameter and with a wall thickness of $1/20$ inch. Fittings could be

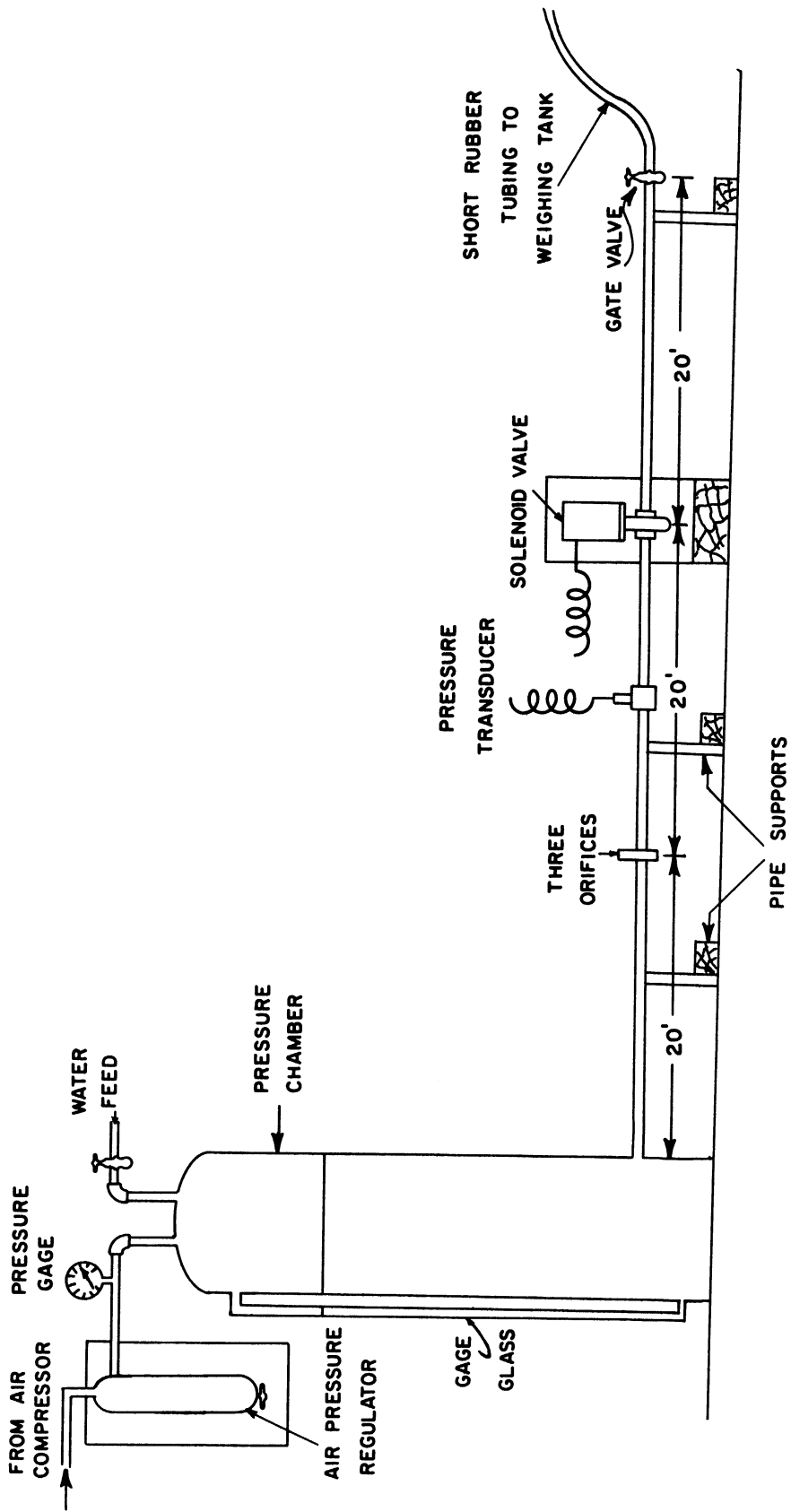


Figure 9. Schematic Diagram of Experimental Set-Up.

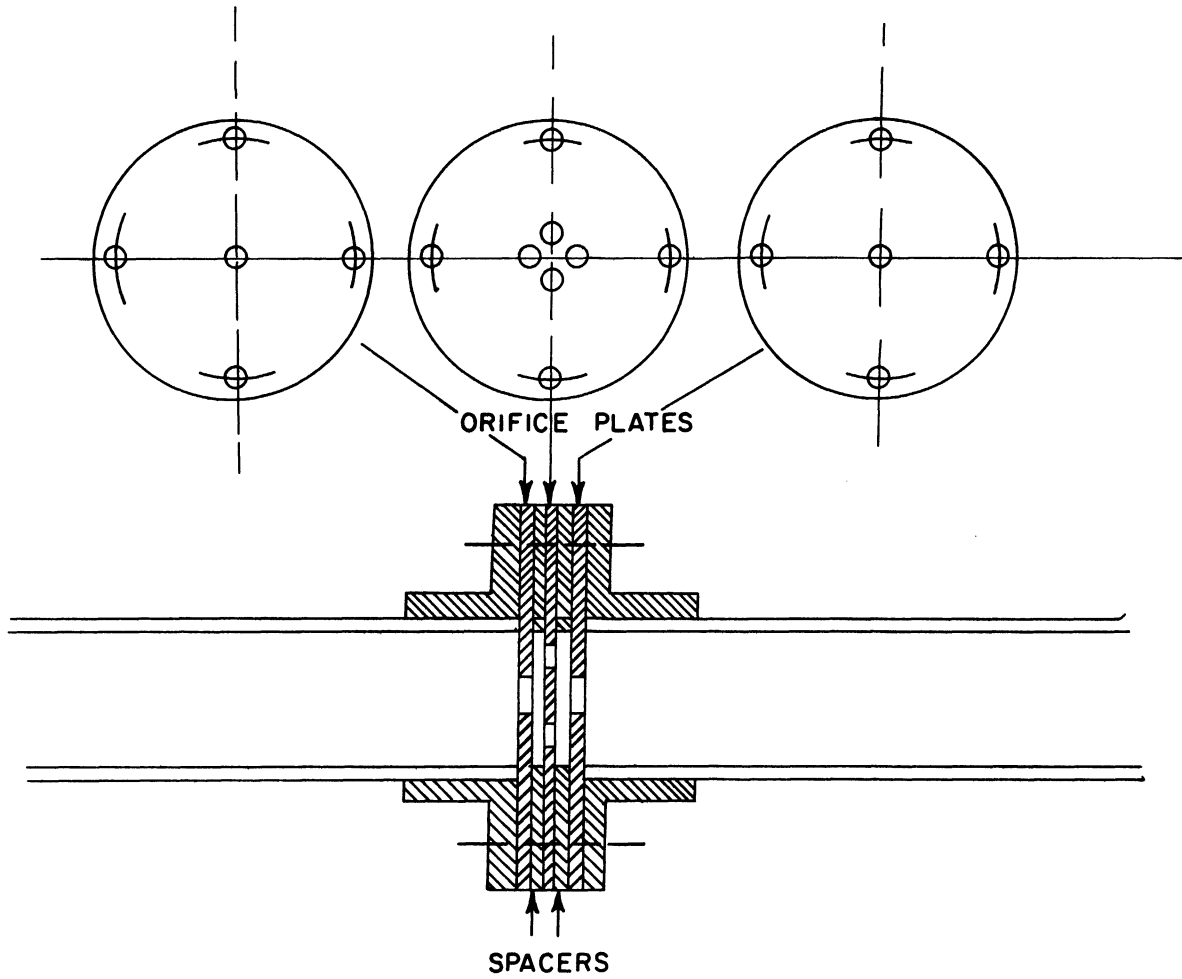


Figure 10. Three Orifices Used in Producing Energy Loss.

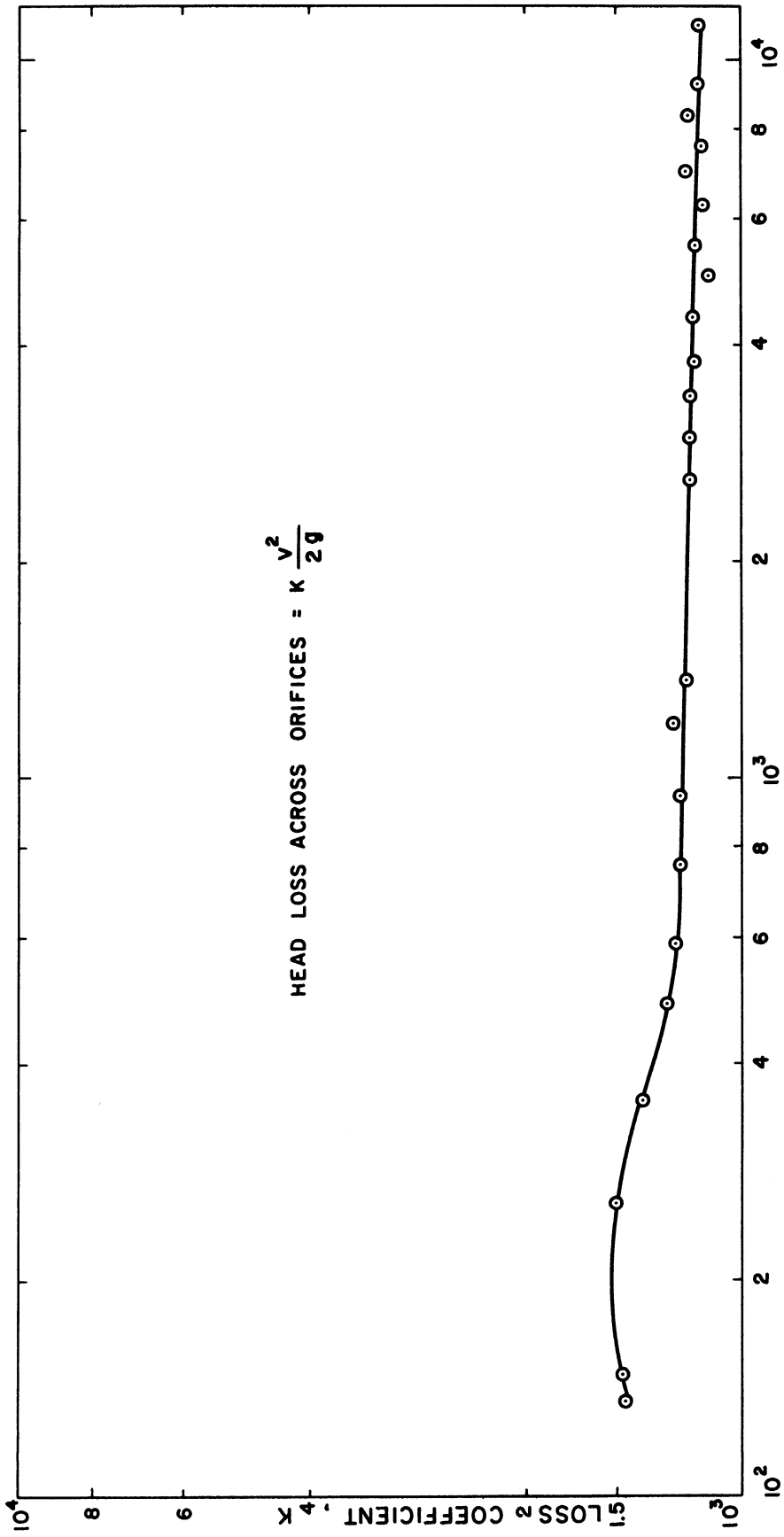


Figure 11. Variation of K vs. R of Three Closely-Spaced Orifices.

connected to it by means of soft-solder. The theoretical wave speed for water in this pipe was 4480 feet per second. Experiments were conducted to determine the Darcy-Weisbach friction factor of the pipe for different Reynolds numbers. From the plot of f versus R , it was seen that, in the turbulent range, the pipe behaved like a smooth pipe and followed Blasius' law, $f = 0.316/R^{1/4}$. As only Reynolds numbers less than 10^5 were expected in the experiment, it was felt that this equation would suffice. For laminar flow, the points closely followed the law $f = 64/R$.

Forty feet from the pressure chamber a solenoid valve was connected to the pipeline. This valve was of the normally closed type. It opened under the action of the solenoid and closed under the action of a coil spring. It was necessary to determine the characteristics of the valve, such as the rate and time of closure and the variation of the hydraulic resistance of the valve as it closed.

The hydraulic resistance of the valve was determined by measuring the pressure drop across the valve as the sliding gate of the solenoid valve was depressed in small steps by means of a screw arrangement attached to the top of the valve. Thus, the variation of τ with displacement of the valve was obtained. The other characteristic of the valve to be determined was the rate and time of closure of the valve. This was done by means of a metallic cantilever beam. The free end of the cantilever was attached to the solenoid bit. Close to the fixed end of the cantilever, two strain gages were glued on, one to the upper side and the other to the lower side of the beam. These two strain gages formed two arms of a Wheatstone bridge. The

output of this bridge was amplified and recorded by a polaroid camera from the screen of an oscilloscope. Calibration of the bridge was performed by depressing the solenoid by known displacements. Recordings were then made as the valve was closed with water in the pipeline. It was seen that the valve opened under solenoid action in about 8.0 milli secs. When closing, it took about 10.0 milli secs. for the solenoid to de-energize and another 12.0 milli secs. for the spring to close the valve.

Combining these two characteristics of the valve, it is possible to determine the τ -versus-time curve for the valve. Comparing the time of closure of the valve (12 milli secs.) with the return-travel time of the valve ($2L/A = 18.0$ milli secs.), it can be seen that we have a case of rapid closure of the valve. The τ -versus-time curve is presented in Figure 12.

Twenty feet downstream from the solenoid valve, the pipeline ends in a gate valve. This valve is operated in such a way as to elevate the static pressure in the pipeline and keep the velocity of the water low. This additional twenty feet of pipe was felt necessary to prevent any reflections from downstream travelling past the solenoid valve whilst it was closing. In this way, the pressure wave in the main pipeline was kept free of any extraneous disturbances.

The discharge from the pipeline was measured gravimetrically. The water was allowed to accumulate in a tank resting on a weighing scale. The time required for a fixed weight of water to be discharged into the tank was determined with the help of a stop watch.

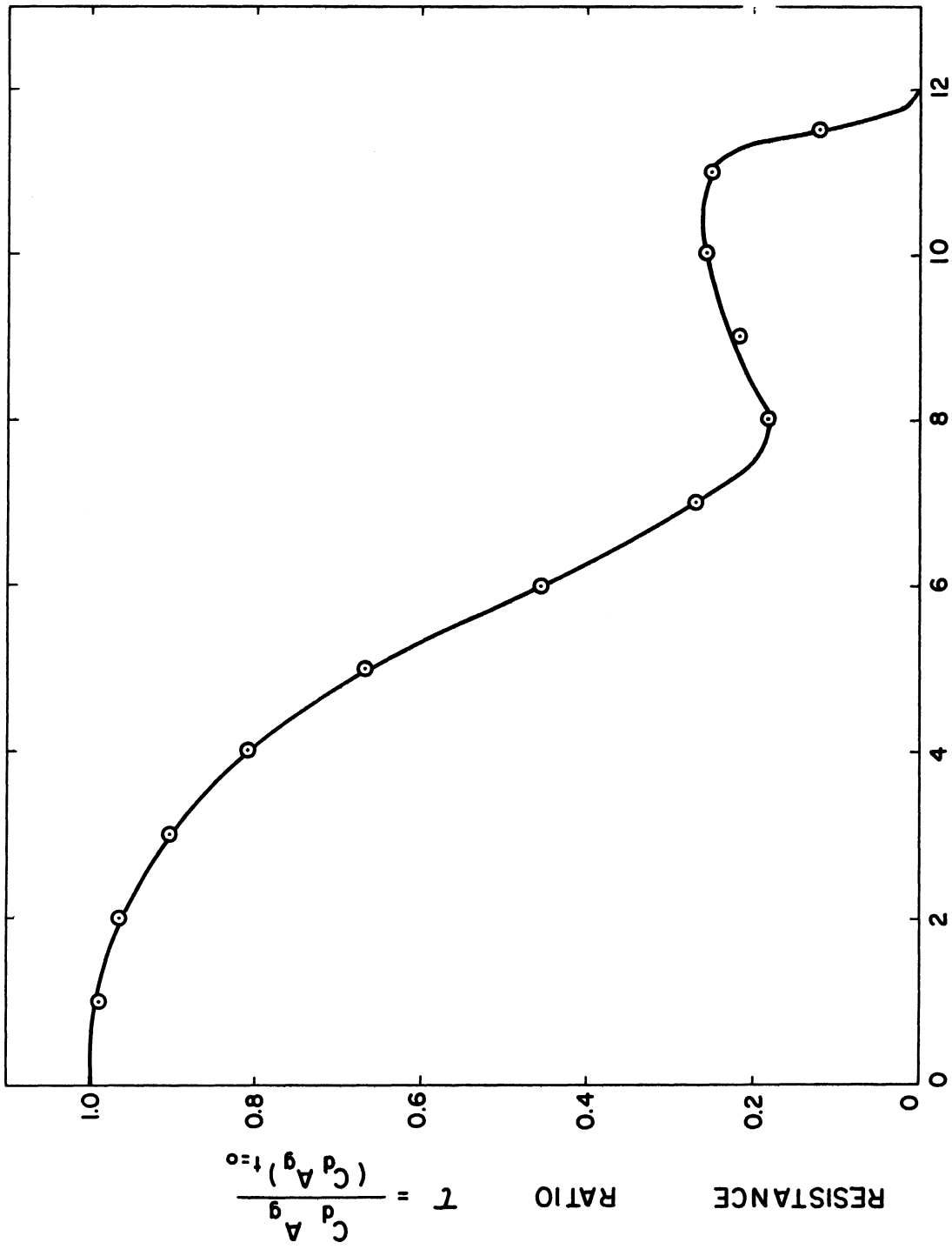


Figure 12. Resistance of Solenoid Valve During Closure.

The pressure sensing device used was a Dynisco pressure transducer. The transducer was attached to the pipeline in such a way as to make the sensitive face of the transducer tangential to the inside circumference of the pipe. The transducer was connected to an Ellis bridge amplifier, which provided the input for the Wheatstone bridge in the transducer and which amplified the output. The bridge amplifier had an outlet for connection to an oscilloscope. The oscilloscope used was a Tektronix model. An attachment on it made it possible to mount a Du Mont camera in front of the screen and photograph traces on polaroid film. Brief specifications of the three pieces of equipment mentioned above are given below.

Dynisco Pressure Transducer.

Model No. PT25-1.5C

Pressure Range. 0-150 psi. Safe Overload. 2x Full Scale

Natural Frequency. 12500 cps.

Configuration. 4 Active Arm Wheatstone Bridge.

Bridge Resistance. 350 ohms \pm 10%.

Ellis Associates Bridge Amplifier and Meter. Model BAM-1

The unit consists of a DC powered bridge circuit, DC transistor amplifier and static and dynamic output connections. By connection to a DC cathode ray oscilloscope, it measures dynamic signals over a frequency range of 0-20000 cps. Resistance transducers, 50-2000 ohms, with 2 or 4 external bridge arms could be used.

Tektronix Dual-Beam Oscilloscope. Type 502

Frequency Response at 5 mV/cm -- 200 kc.

Triggering signal sources -- Upper beam, lower beam, external or line.
Internal triggering -- a signal producing 2 mm vertical deflection on either lower or upper beam.

External triggering -- 0.2 to 10 volts on either polarity.

The oscilloscope was capable of being triggered in several ways. It was necessary for this experiment to trigger the trace in two different ways. First, use was made of a microswitch, depressing which a single trace would travel across the screen. This method was used for registering the constant pressures before and after closure of the solenoid valve. The other arrangement triggered a trace by the use of the same switch which operated the solenoid valve. This method was used to trigger the water-hammer pressure wave.

The sweep rate of the oscilloscope could be adjusted in steps from 5 secs/cm to 200 μ secs/cm. Two sweep rates were most satisfactory for these experiments. First, when registering only one cycle of the wave on the screen, a sweep rate of 5 milli-secs/cm. was used. However, when four cycles of the wave were required, 2 photographs were made, each registering 2 consecutive cycles using a sweep rate of 10 milli-secs/cm. The accuracy of these sweep rates was checked by means of an audio oscillator. It was found that there was an error of about 6% in the sweep rates and so the actual time scales on the photographs were 1 cm. = 4.7 milli secs. and 1 cm. = 9.4 milli secs.

The camera mounted on the oscilloscope was a Du Mont Oscilloscope Camera Type 450. A few adjustments had to be made before good, clear photographs could be taken with it. First of all, the back

of the polaroid camera was opened up and a ground-glass plate taped exactly where the film would be held. A steady trace was produced on the screen by means of an audio oscillator. This trace was brought into focus on the ground-glass plate by means of the focussing knob. This position of the knob was marked, so that it could be brought back to this position at a later time. In this position, it was seen that the graticule was not in focus since the graticule and the screen are not in the same plane. Hence, after illuminating the graticule, it was brought into focus on the ground glass plate and this position of the focussing knob was also marked. For clear, well-focussed pictures, these two different positions had to be used when photographing the graticule and traces on the screen.

Photographs of the experimental set-up and the instruments are presented in Plates I to IV, on pages 42 and 43.

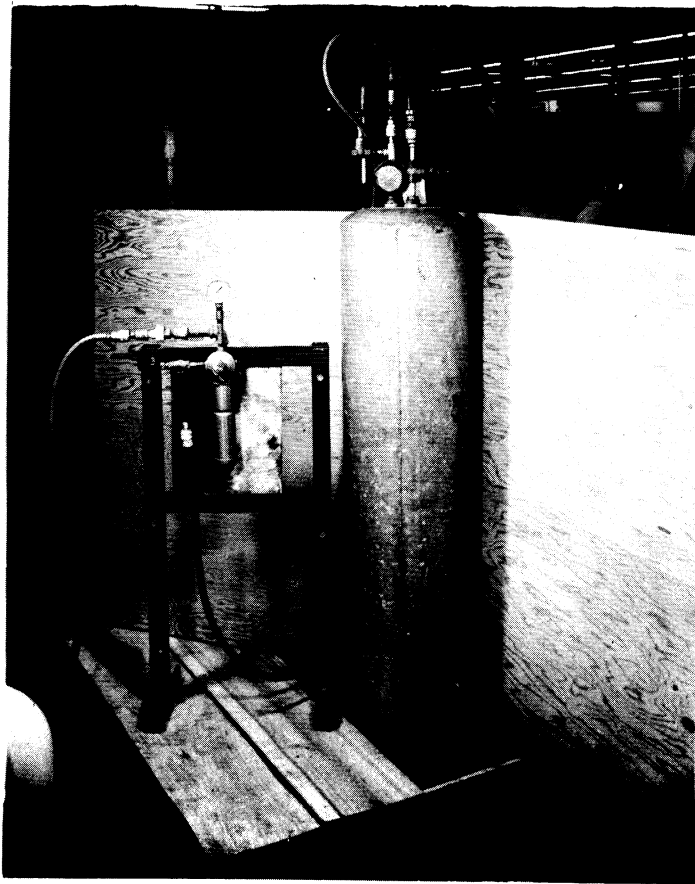


Plate I. Compression Chamber and Air Pressure Regulator.

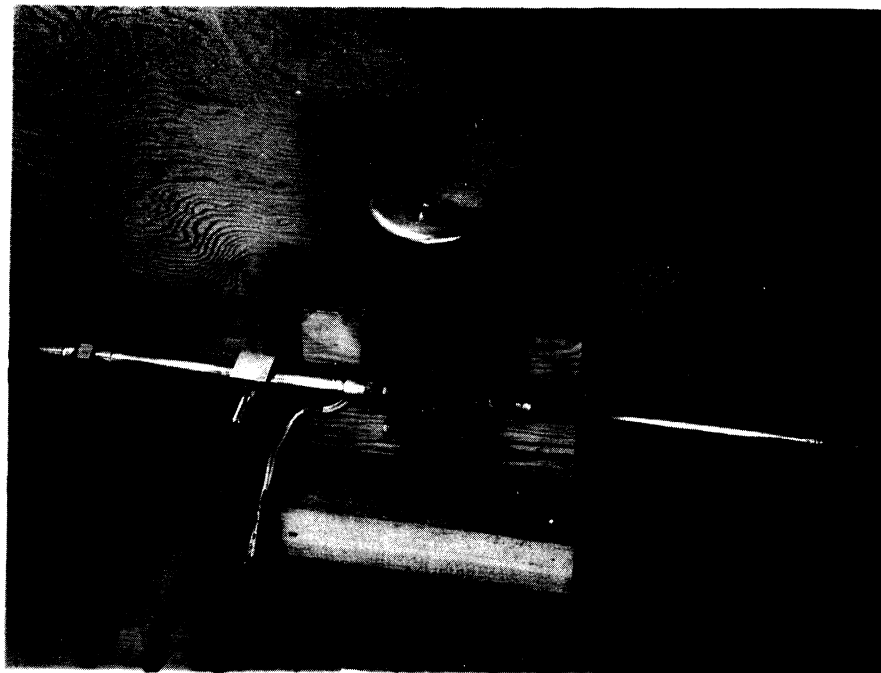


Plate II. Solenoid Valve and Pressure Transducer.

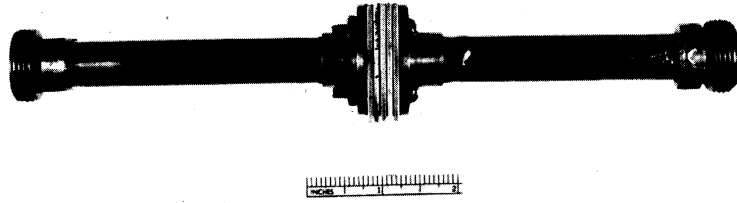


Plate III. Closely-Spaced Orifices Used to Produce Energy Loss.

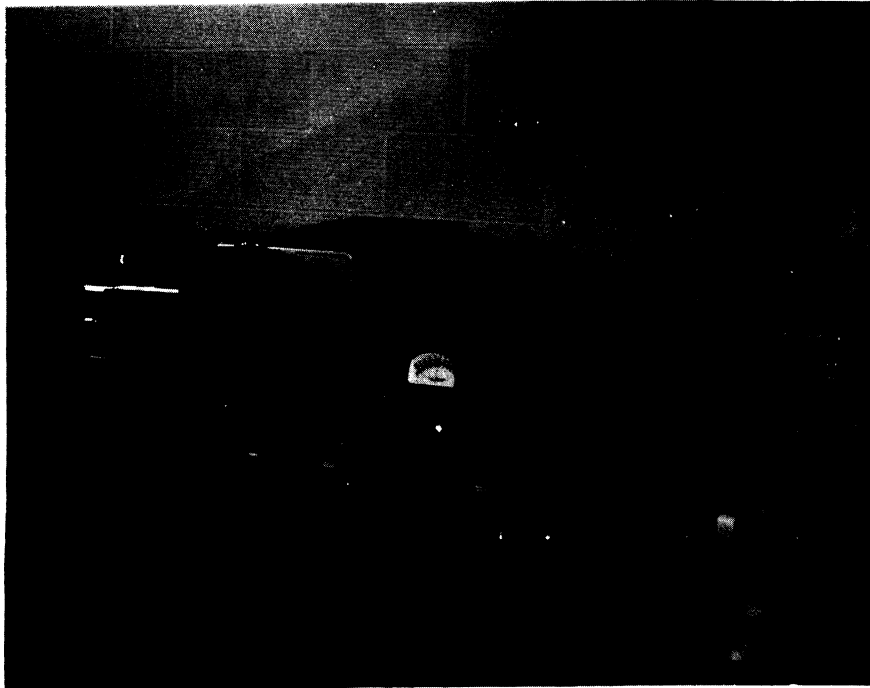


Plate IV. Recording and Calibrating Instrumentation.

VI. EXPERIMENTAL PROCEDURE

The following different experiments were conducted.

- 1) Pipeline with a Minor Loss in the Middle.
 - a) Turbulent Flow. Pressure transducer at $x' = 40$ ft.
 - b) Turbulent Flow. Pressure transducer at $x' = 30$ ft.
 - c) Laminar Flow. Pressure transducer at $x' = 40$ ft.
 - d) Laminar Flow. Pressure transducer at $x' = 30$ ft.

- 2) Straight Pipeline.
 - a) Turbulent Flow. Pressure transducer at $x' = 40$ ft.
 - b) Turbulent Flow. Pressure transducer at $x' = 30$ ft.
 - c) Laminar Flow. Pressure transducer at $x' = 30$ ft.

Each of these experiments followed the same procedure, which will be described below. First of all, the electronic instruments were switched on and allowed to warm up for an hour or more, so that there is no drift in the trace. Next, the pressure chamber was filled with water and the air pressure regulator set to a constant pressure at about 80 psi. With the solenoid valve open, the gate valve is regulated so that the required velocity in the pipe is obtained. This is accomplished by trial and error. The required velocity in the pipe was chosen so that the pressure in the pipe did not at any time of the experiment fall below atmospheric pressure. This was to reduce all chances of water column separation.

With the electronic instruments warmed up, the pressure transducer was connected to a dead-weight gage tester. Dead weights

equivalent to a pressure of 90 psi were applied and the vertical deflection of the beam on the oscilloscope adjusted to be exactly 3 cm. In this way, a pressure scale of 1 cm. = 30 psi was obtained. The transducer was then connected to the appropriate place in the pipeline. Every effort was made to remove all the free air that may have been trapped in the pipeline. This was accomplished by letting the water flow in the pipeline with a high velocity for a sufficiently long time.

The time scale on the oscilloscope was adjusted so that one or two cycles of the pressure wave were accommodated on the screen. The intensity of the beam was adjusted so that it was not too bright and yet all the fine details of the wave registered on the photograph. The camera was now attached to the oscilloscope. The screen was brought into focus and the lens opening increased to its maximum value. The shutter-timing mechanism was set to the 'bulb' position. With the shutter lever depressed, a trace was triggered across the screen by pressing the micro-switch. This straight line represented the static pressure at that point under steady-state conditions. Then, the switch operating the solenoid valve was closed and another trace was thereby triggered across the screen. This was the water-hammer pressure versus time curve. The third trace to be triggered across the screen was the constant pressure H_0 causing the flow. The last thing to be done was to illuminate the graticule, bring it into focus, reduce the lens opening to $f = 11$, adjust the shutter time to be $1/25$ second and depress the shutter release. This provided a background of horizontal and vertical lines spaced one cm. apart in both directions.

These lines were helpful when transferring the trace on the photograph to another graph. The polaroid film was then developed in the 10 secs. coated with the permanentizing solution and was ready for comparing with the theoretical curve.

VII. THE COMPUTER PROGRAM

The computer program was written for an IBM 7090 computer installed at the University of Michigan Computing Center. The language in which the program has been written is known as the Michigan Algorithm Decoder,⁽⁹⁾ or in short, the MAD Language. A flow diagram, illustrated in Figure 13, indicates the procedure used in the program. It also helps to break up the long program into short and simple parts which make it easier to understand.

The main steps in the program are as follows; reading-in the data, setting up of function subroutines, calculation of certain constants, setting up the initial values in the pipe and calculation of pressure and velocity for as long a time as may be desired. The last part is the real core of the program. It is broken up into two parts. The first part involves the calculation of V and H for time t less than t_c and the other part of time t greater than t_c . When the time t exceeds a specified limit, the program is terminated. Three function statements are defined at the beginning of the program. The first determines the friction factor f for a given velocity. The second determines the loss coefficient of the orifice for a given velocity. The last function determines the head and velocity at a boundary condition, involving a minor loss. This last function is called upon in the main part of the program by means of an "Execute Function" Statement.

The program and a part of the program output is given in Appendices I and II. The head and velocity in the pipeline at 5-foot intervals are printed out, even though calculations were made at intervals of one foot.

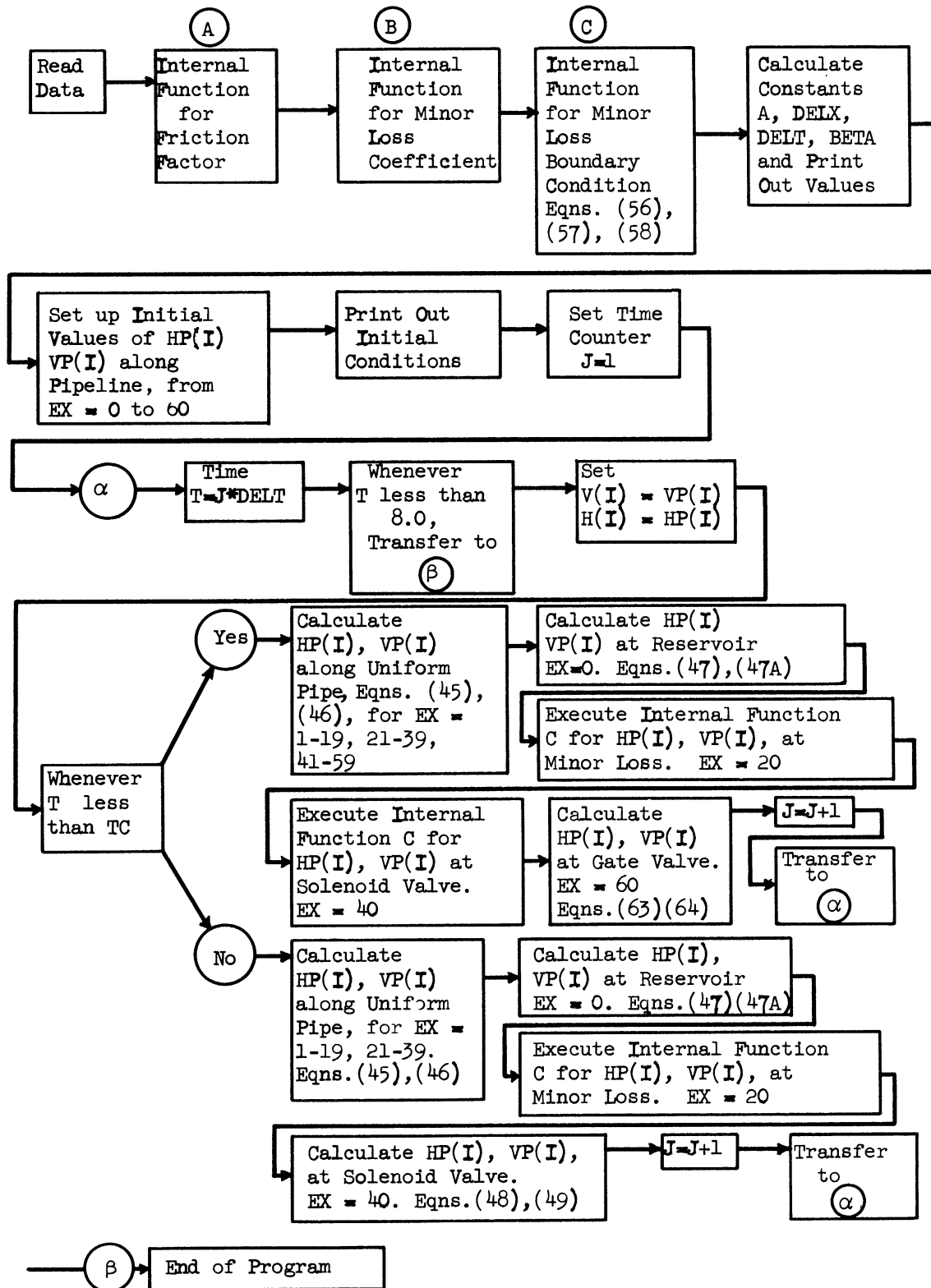


Figure 13. Flow Diagram for Computer Program.

VIII. DISCUSSION OF RESULTS

The results of the experiments are shown in their original photographic form in Plates (V) to (XIII), on pages 50 through 58. Comparisons of the experimental and theoretical wave forms can be made in Figures 14 to 22. For all cases, four cycles of the pressure wave have been reproduced. In addition to this, pressure-time diagrams of one cycle have also been presented for the case of the pipeline with a minor loss in the middle. In this way it is possible to see the magnitude of the reflection in the one-cycle diagram and also observe its influence on the decay of the pressure wave in the four-cycle diagram.

It was the intention of the author to obtain a wave form with as few disturbances as possible so that the reflection of the wave could be noticed easily. It was for this reason that a pump was not used at the upstream end and instead a compression chamber with compressed air was thought necessary. However, there were some disturbances that could not be eliminated. The way in which the solenoid valve closed, produced one such disturbance that appears in every cycle of the wave and was taken into account in the theoretical program.

It can be seen that in every case, the experiment and theory agree in the first half of the first cycle. There is agreement both in magnitude and form of the wave. In Figures 14 and 16 the reflection from the minor loss can be seen and compared with the steady-state minor loss. Thus, the validity of Equations (56), (57), (58) and hence of Equations (13) and (15) is upheld. It is only in this part of the

PIPE WITH MLOSS

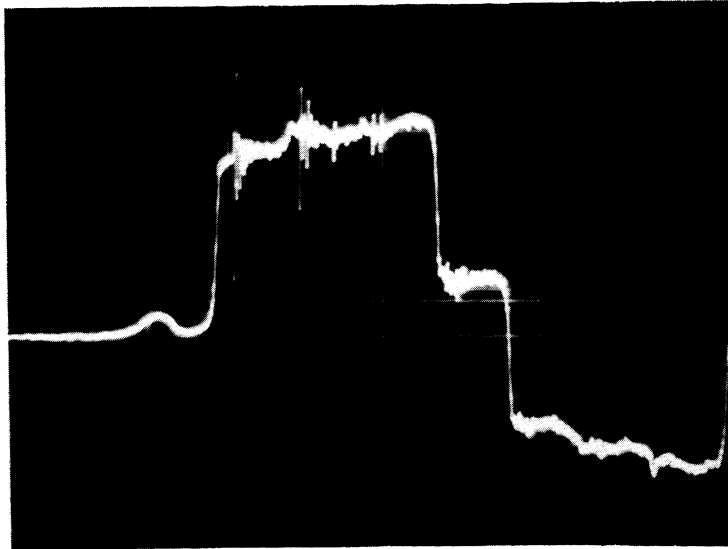
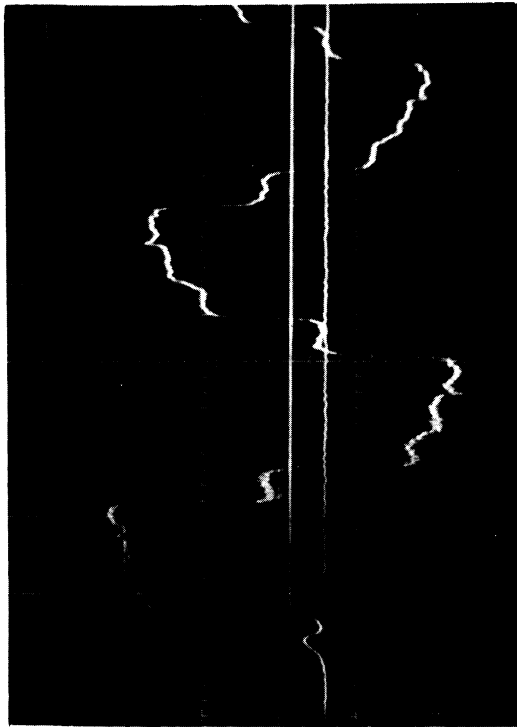


Plate V. Water-Hammer Pressure-Time Diagram.

Case 1(a), 1 cycle
Temp. = 78°F
HO = 194'

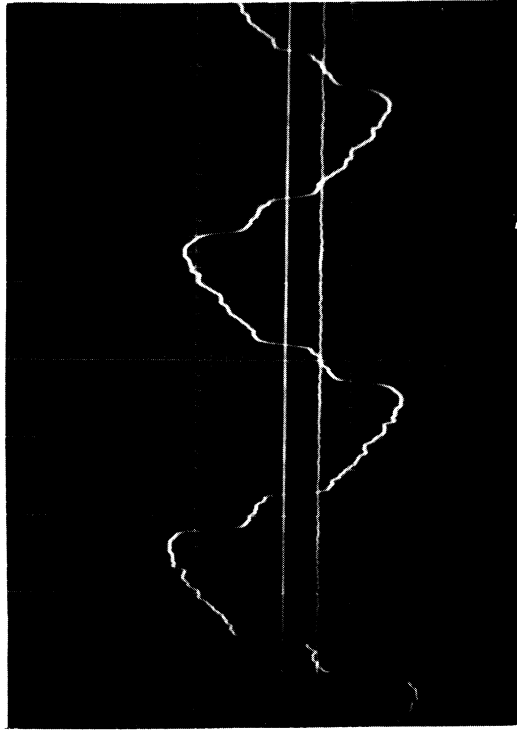
$V_0 = 1.20' / \text{sec}$
Pressure Scale 1 cm = 30 psi
Time Scale 1 cm = 5 m.secs.

PIPE WITH MLOSS



1

PIPE WITH MLOSS



2

Plate VI. Water-Hammer Pressure-Time Diagram.

Case 1(a) 4 cycles
Temp. = 78°F
HO = 1940'

VO = 1.2'/sec
Pressure Scale 1 cm = 30psi
Time Scale 1 cm = 10 m.secs.

PIPE WITH MLOSS

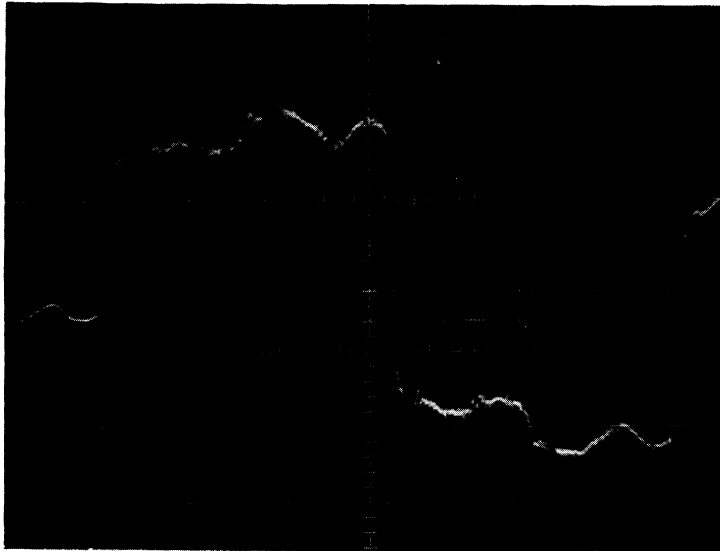
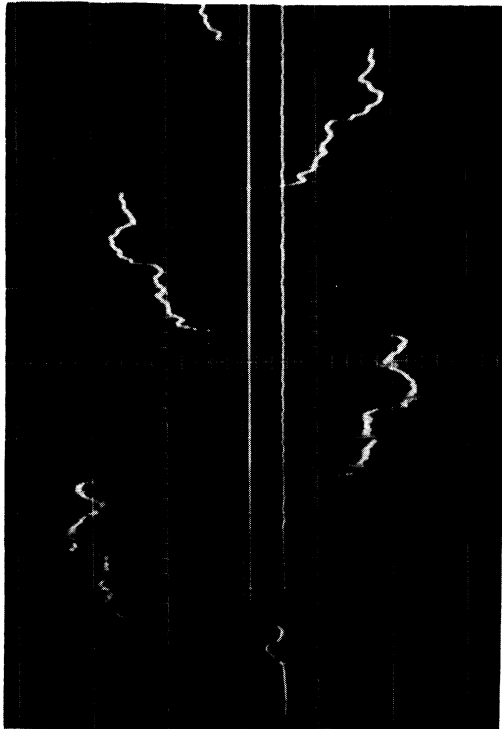


Plate VII. Water-Hammer Pressure-Time Diagram.

Case 1 (b) 1 cycle
Temp. = 75°F
HO = 193'

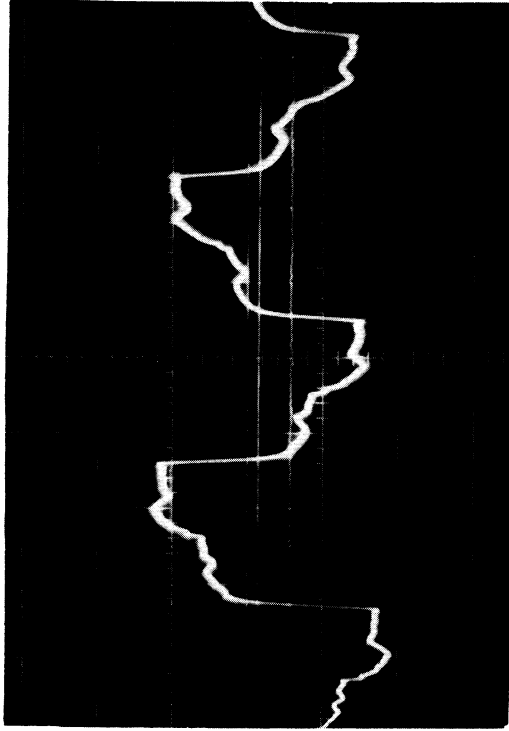
VO = 1.2'/sec.
Pressure Scale 1 cm = 30 psi
Time Scale 1 cm = 5 m.secs.

PIPE WITH MLOSS



1

PIPE WITH MLOSS



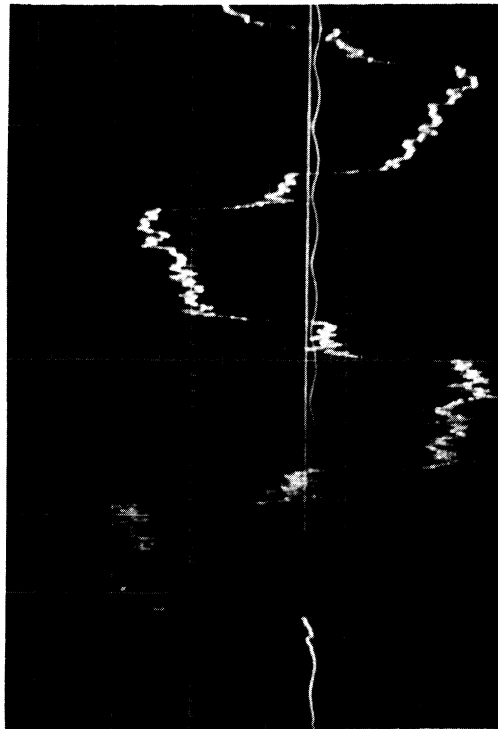
2

Plate VIII. Water-Hammer Pressure-Time Diagram.

Case 1(b) 4 cycles $V_0 = 1.2' / \text{sec}$
 Temp. = 75°F Pressure Scale 1 cm = 30 psi
 HO = 197.0' Time Scale 1 cm = 10 m.secs.

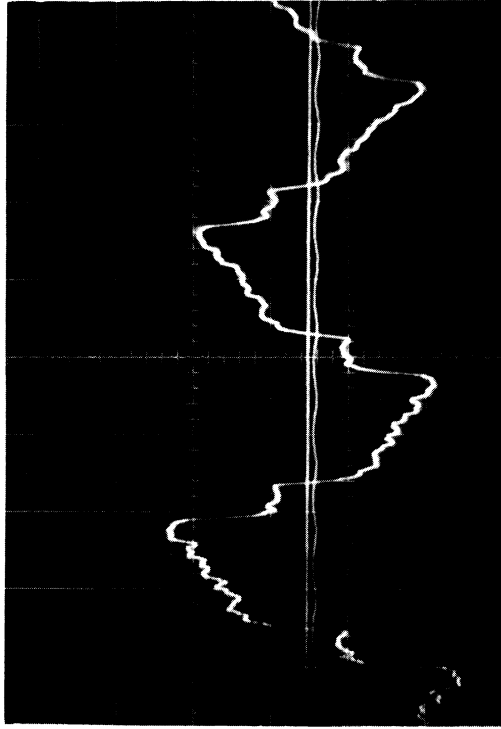
PIPE WITH MLOSS

LAMINAR FLOW



PIPE WITH MLOSS

LAMINAR FLOW



1

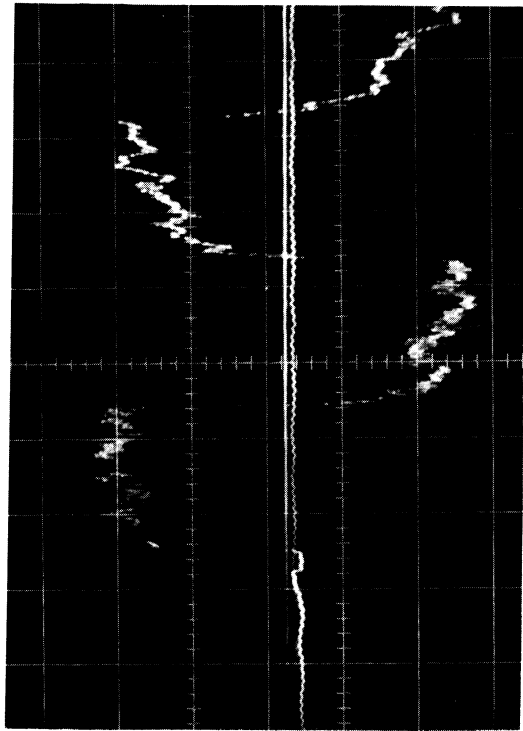
2

Plate IX. Water-Hammer Pressure-Time Diagram.

Case	1(c)	$V_0 = 0.300' / \text{sec}$
Temp.	77°F	Pressure Scale 1 cm = 8 psi
HO	466'	Time Scale 1 cm = 10 m.secs.

PIPE WITH MLOSS

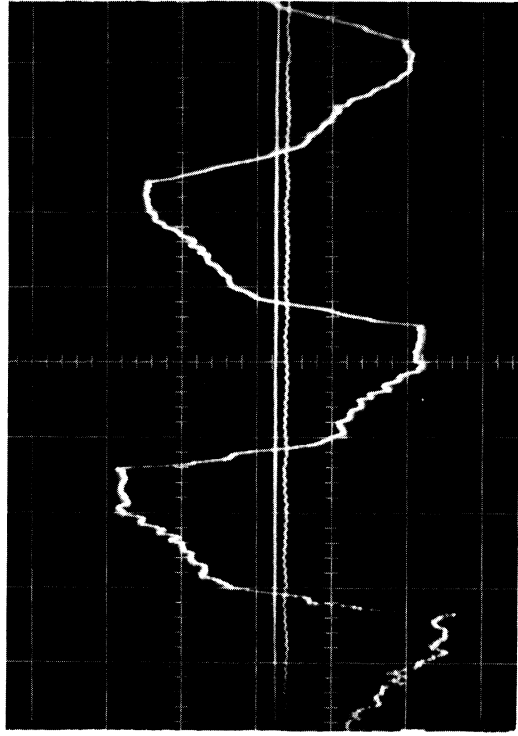
LAMINAR FLOW



1

PIPE WITH MLOSS

LAMINAR FLOW



2

Plate X. Water-Hammer Pressure-Time Diagram.

Case 1(d)

VO = .330'/sec

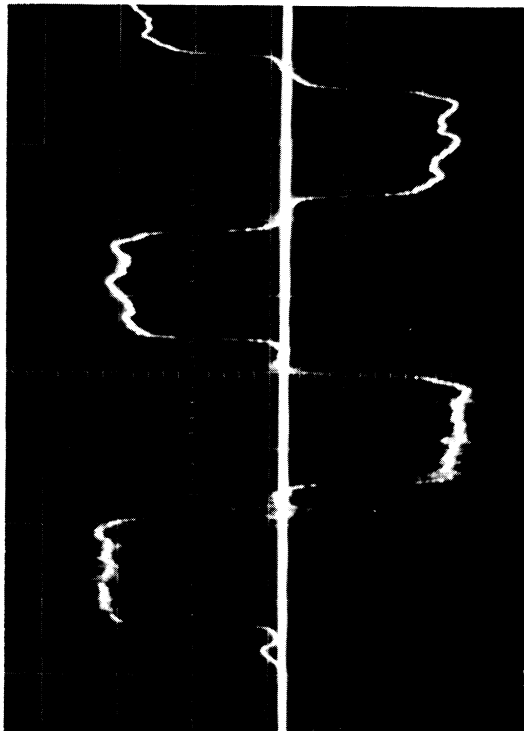
Temp. = 76°F

Pressure Scale 1 cm = 8 psi

HO = 49.0'

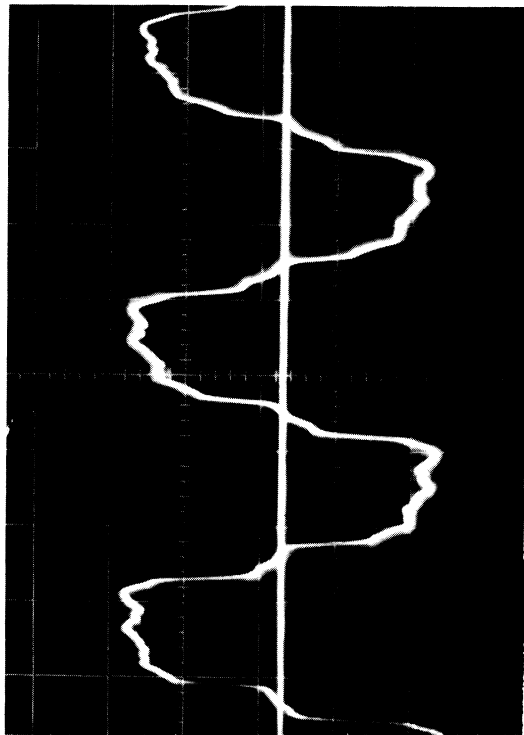
Time Scale 1 cm = 10 m.secs.

STRAIGHT PIPE



1

STRAIGHT PIPE



2

Plate XI. Water-Hammer Pressure-Time Diagram.

Case 2(a)

Temp. = 79°F

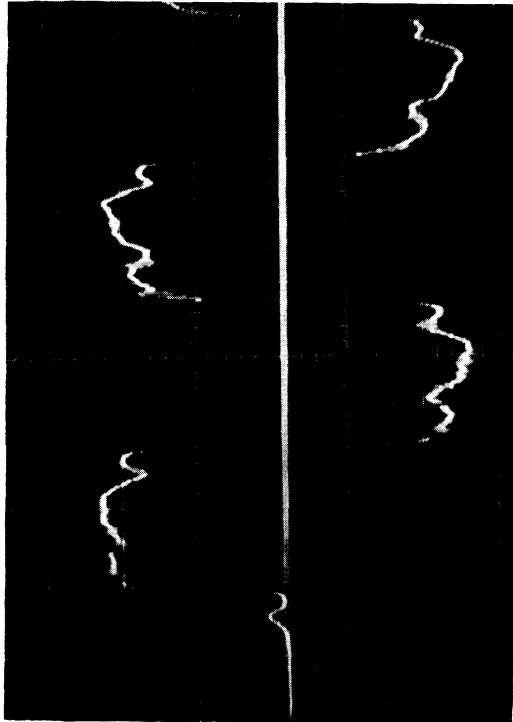
HO = 194.0'

VO = 1.212'/sec.

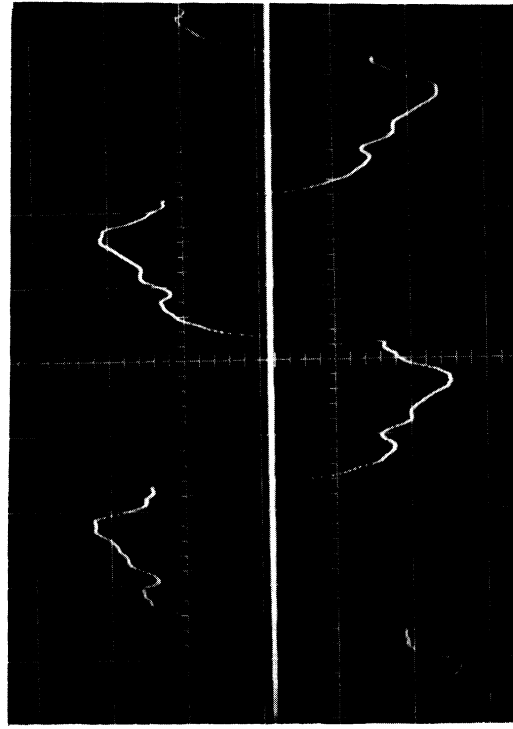
Pressure Scale 1 cm = 30 psi

Time Scale 1 cm = 10 m.secs.

STRAIGHT PIPE



STRAIGHT PIPE



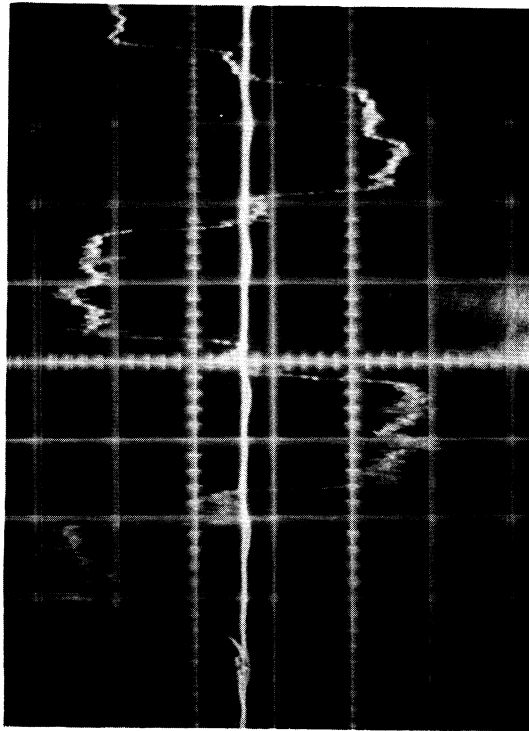
2

Plate XII. Water-Hammer Pressure-Time Diagram.

Case 2(b) $V_0 = 1.20' / \text{sec}$
Temp. = 75°F Pressure Scale 1 cm = 30 psi
HO = 194.0' Time Scale 1 cm = 10 m.secs.

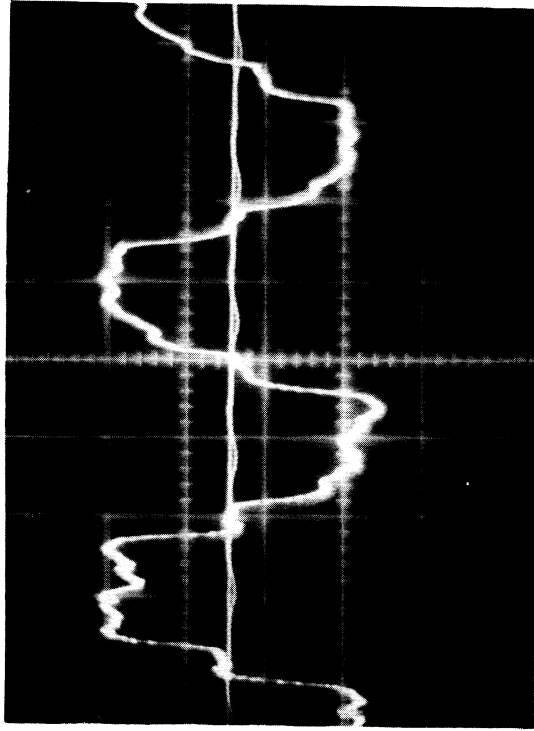
STRAIGHT PIPE

LAMINAR FLOW



STRAIGHT PIPE

LAMINAR FLOW



1

2

Plate XIII. Water-Hammer Pressure-Time Diagram.

Case 2(c)

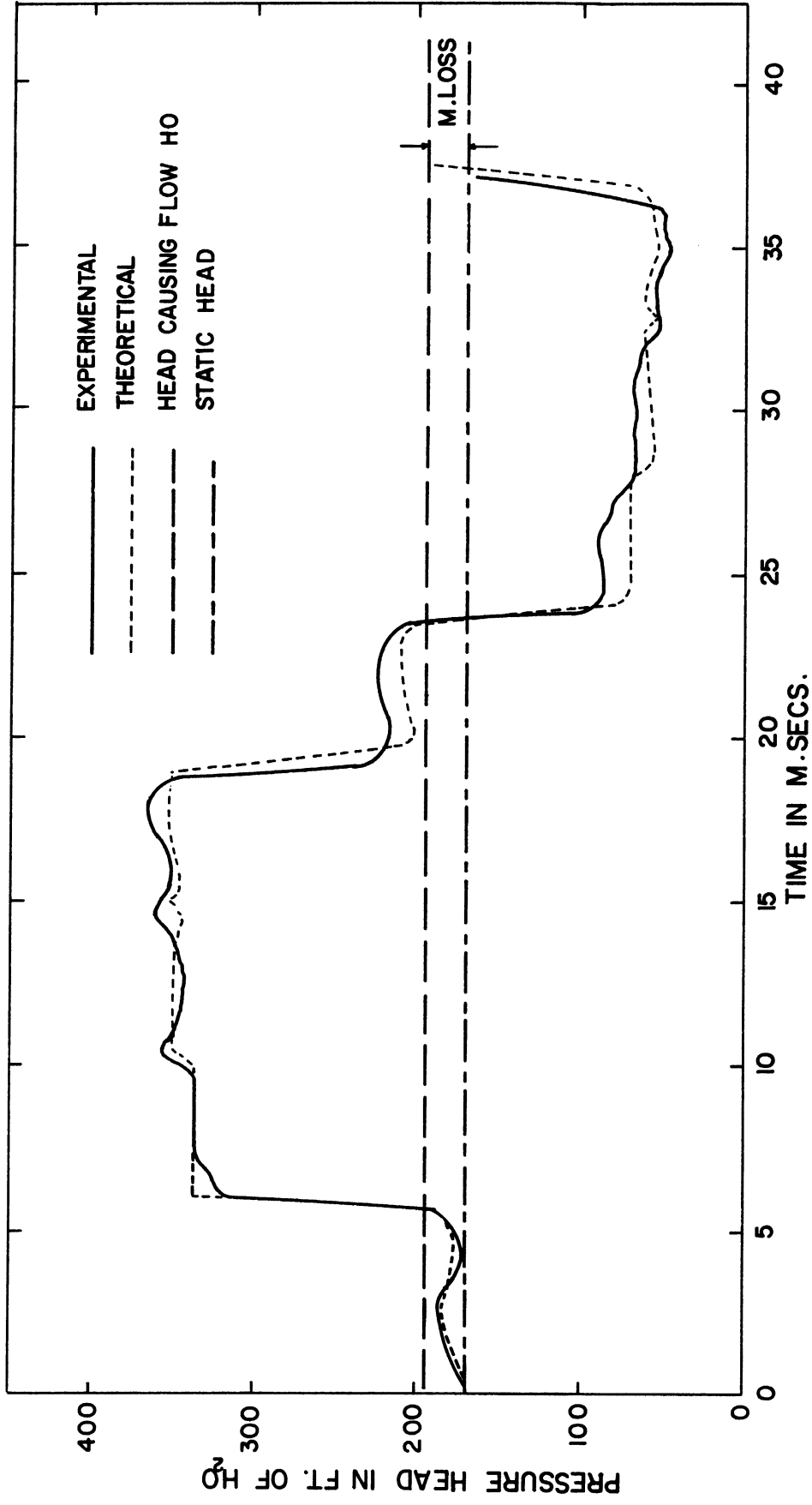
$V_0 = 0.299' / \text{sec}$

Temp. = 77°F

Pressure Scale 1 cm = 8 psi

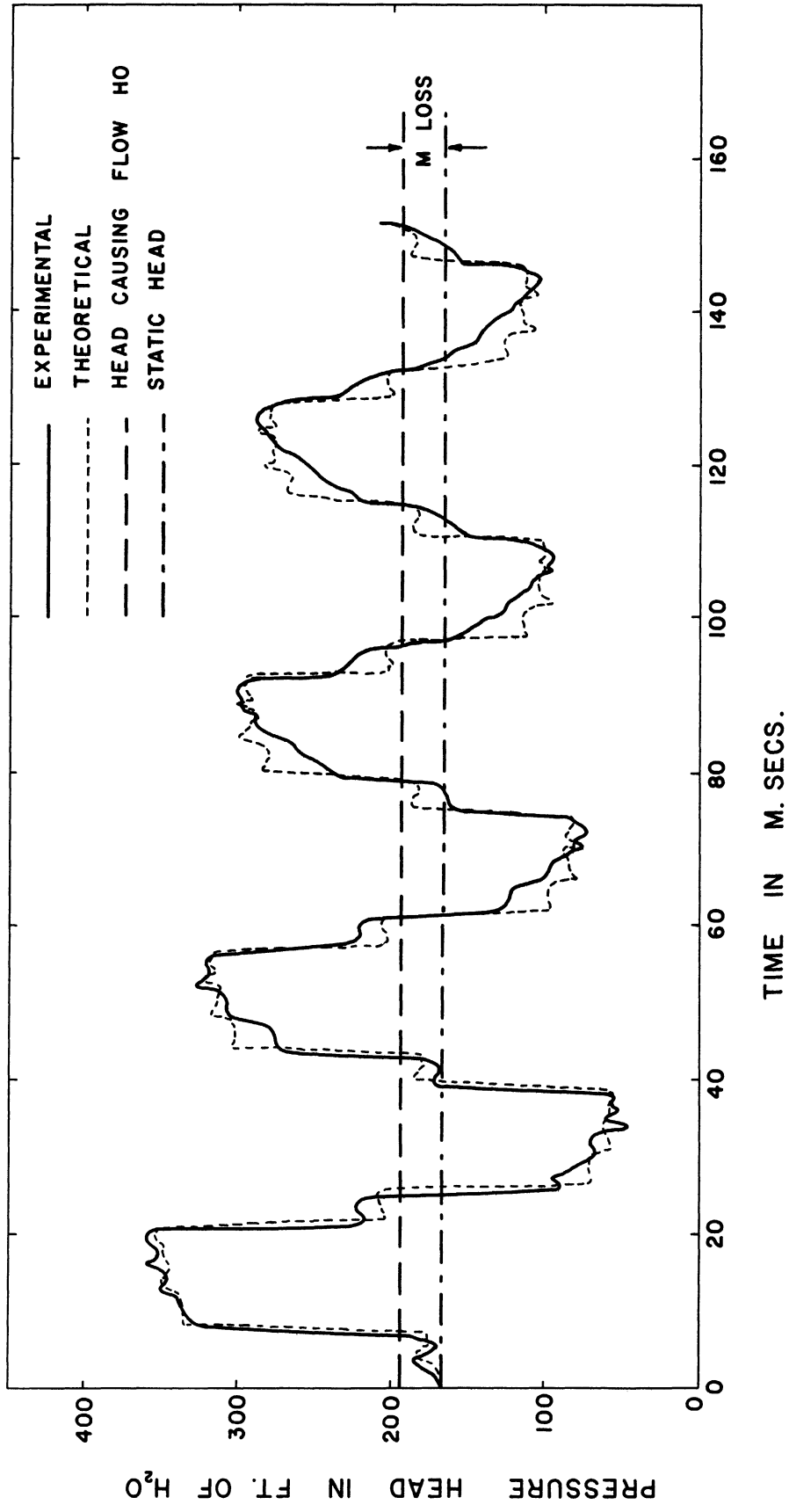
HO = 47.0'

Time Scale 1 cm = 10 m.secs.



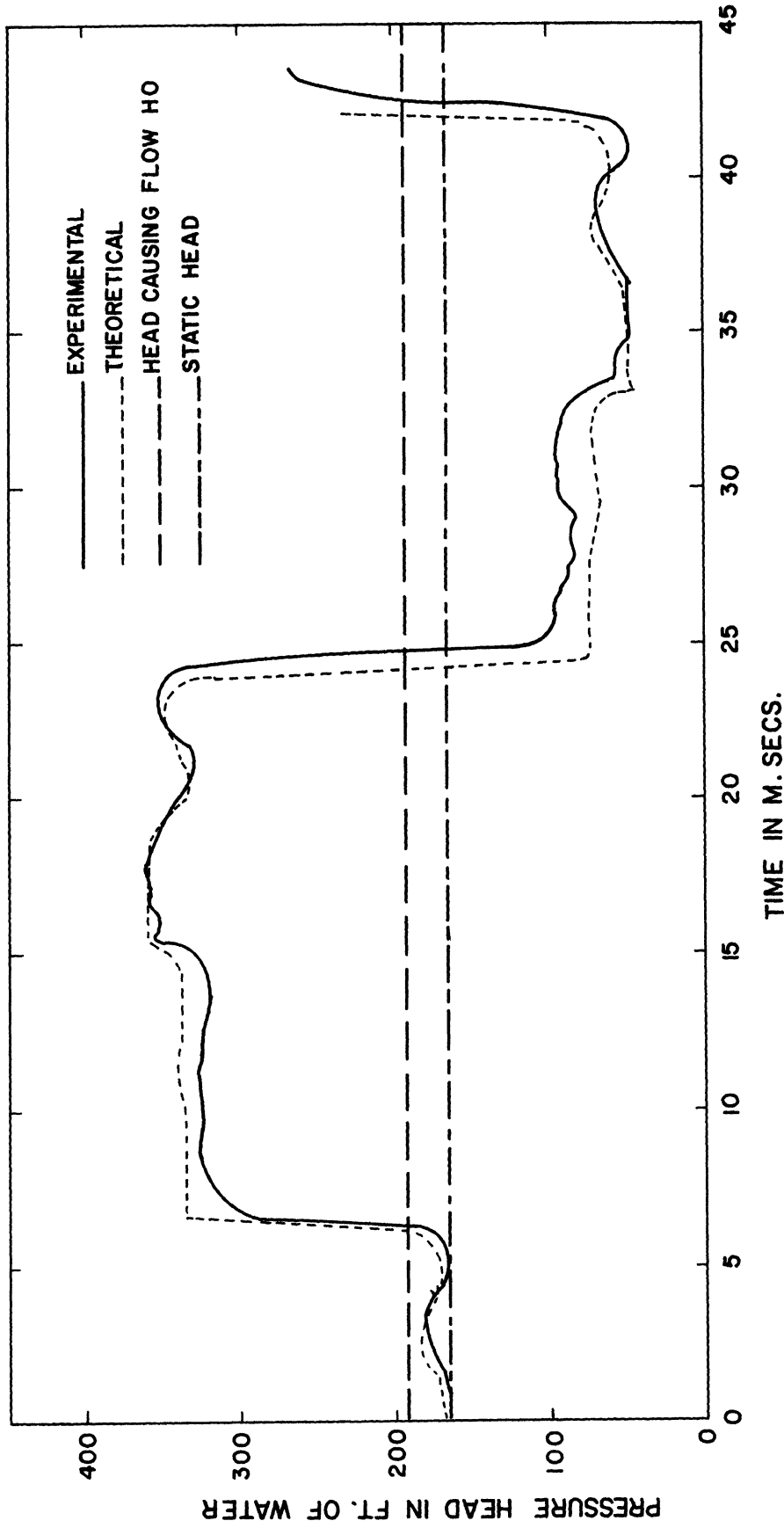
CASE 1(a)

Figure 14. Water-Hammer Pressure-Time Diagram. At $x = 3$ L/4 Pipe with Minor Loss in Middle. Turbulent Flow. $H_0 = 194.0'$; $V_0 = 1.20'$ /sec.; Temp. = 78°F .



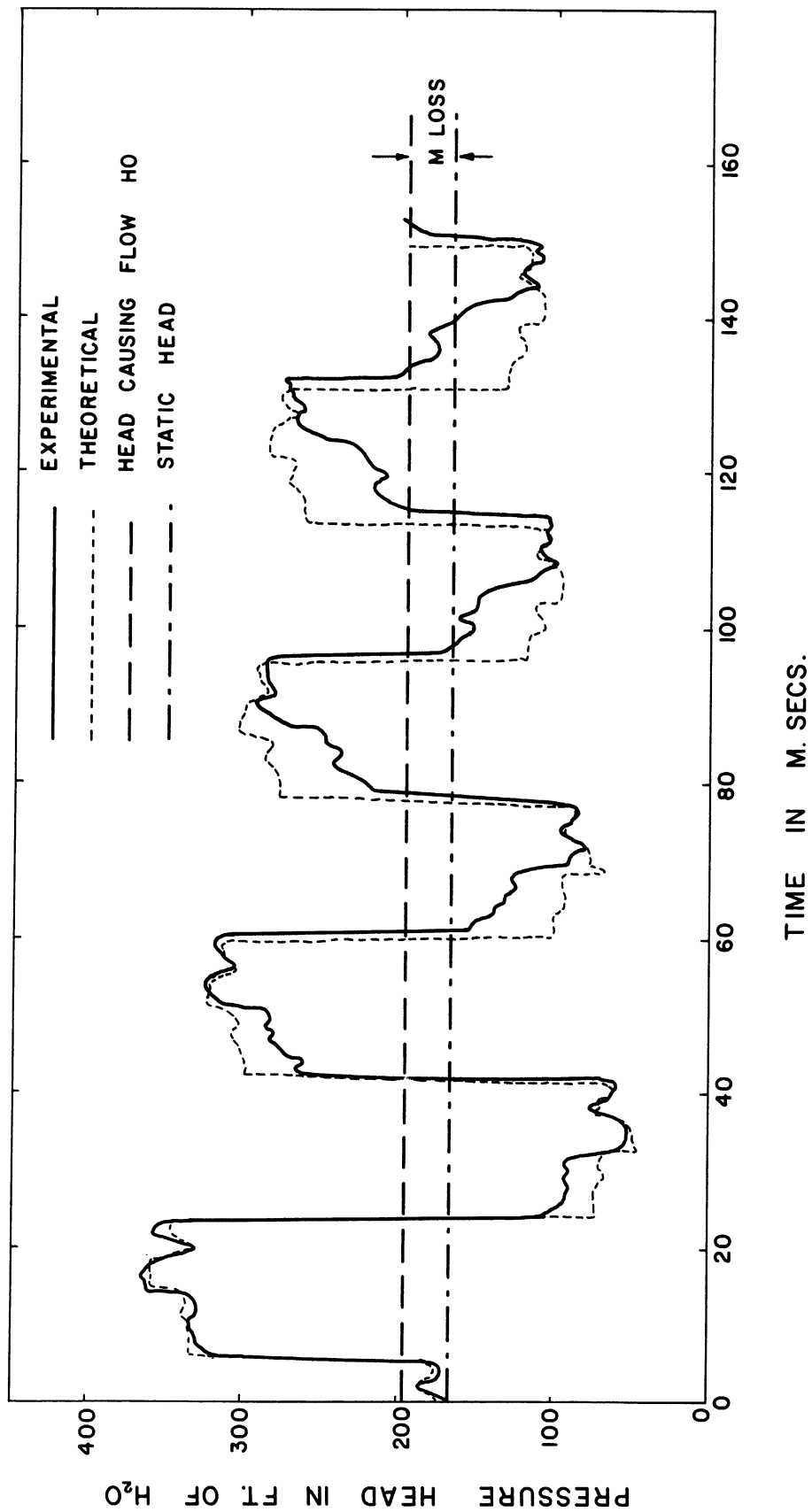
CASE 1(a)

Figure 15. Water-Hammer Pressure-Time Diagram. At $x = 3L/4$ Pipe with Minor Loss in Middle. Turbulent Flow. $H_0 = 194.0'$; $V_0 = 1.20'$ /sec.; Temp. = 78°F .



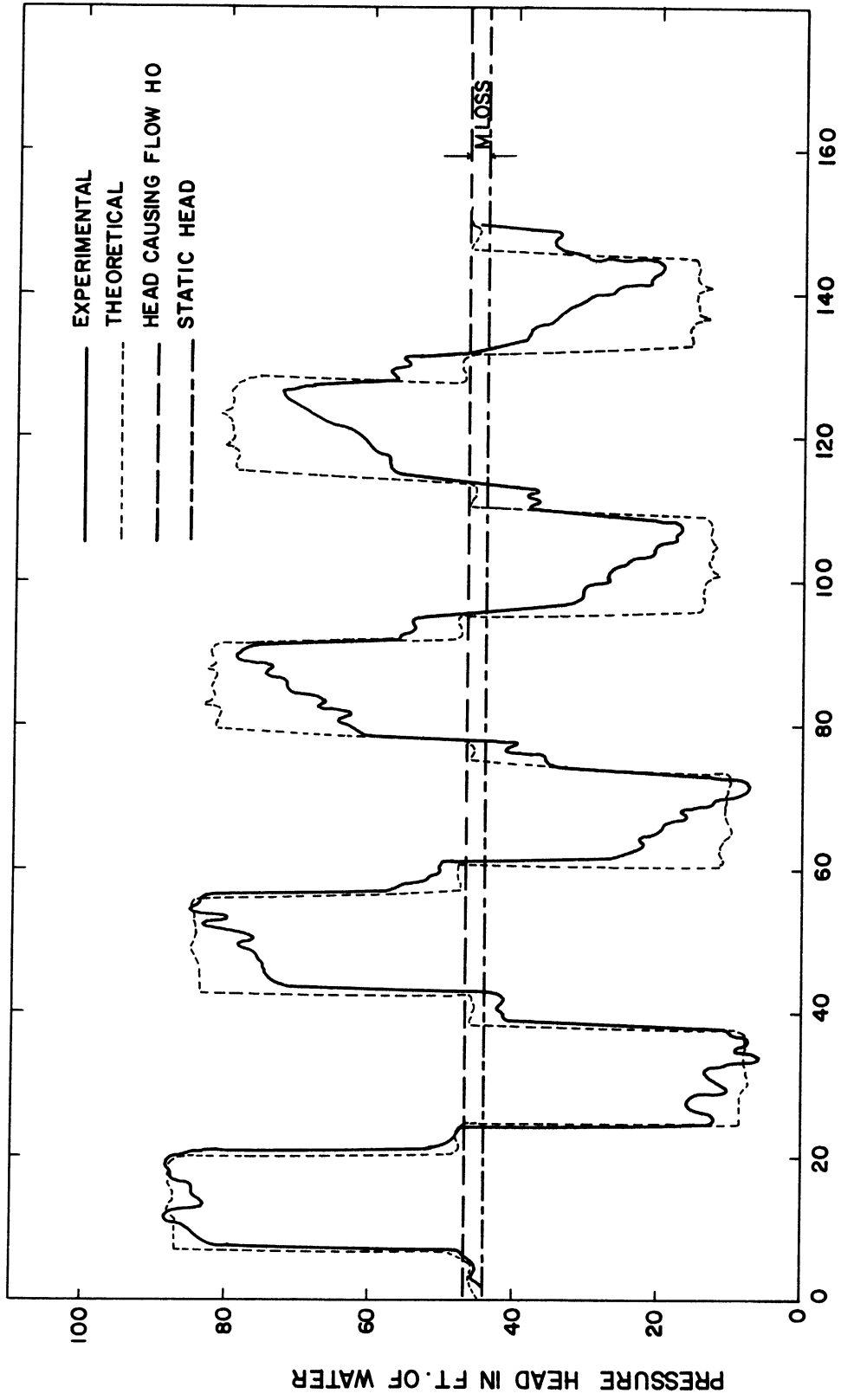
CASE 1(b)

Figure 16. Water-Hammer Pressure-Time Diagram. At $x = L$. Pipe with Minor Loss in Middle. Turbulent Flow. $HO = 193.0'$; $VO = 1.20'$ /sec.; Temp. = $75^{\circ}F$.



CASE 1(b)

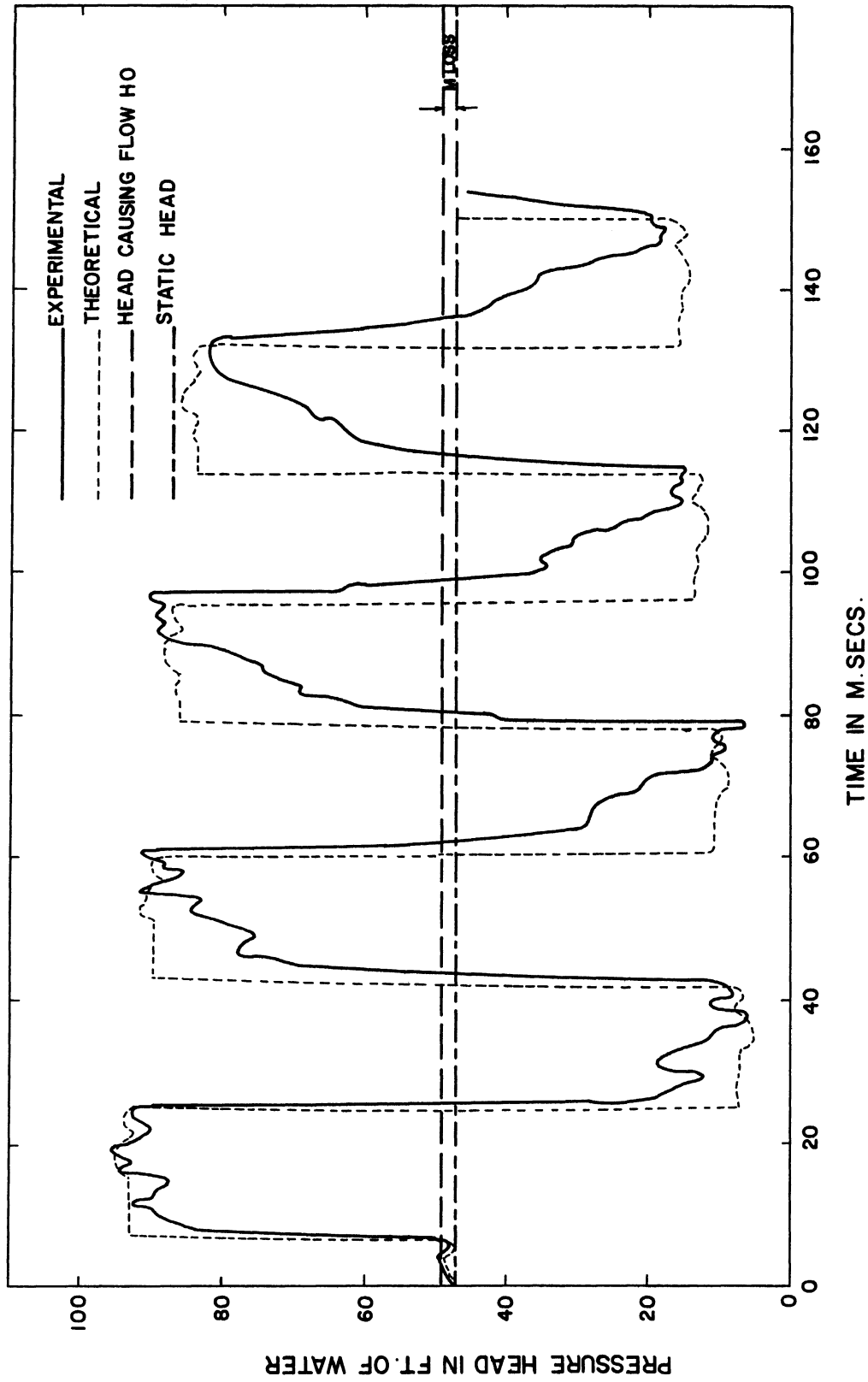
Figure 17. Water-Hammer Pressure-Time Diagram. At $x = L$. Pipe with Minor Loss in Middle. Turbulent Flow. $HO = 197.0'$; $VO = 1.2'$ /sec.; Temp. = $75^{\circ}F$.



TIME IN M. SECS.

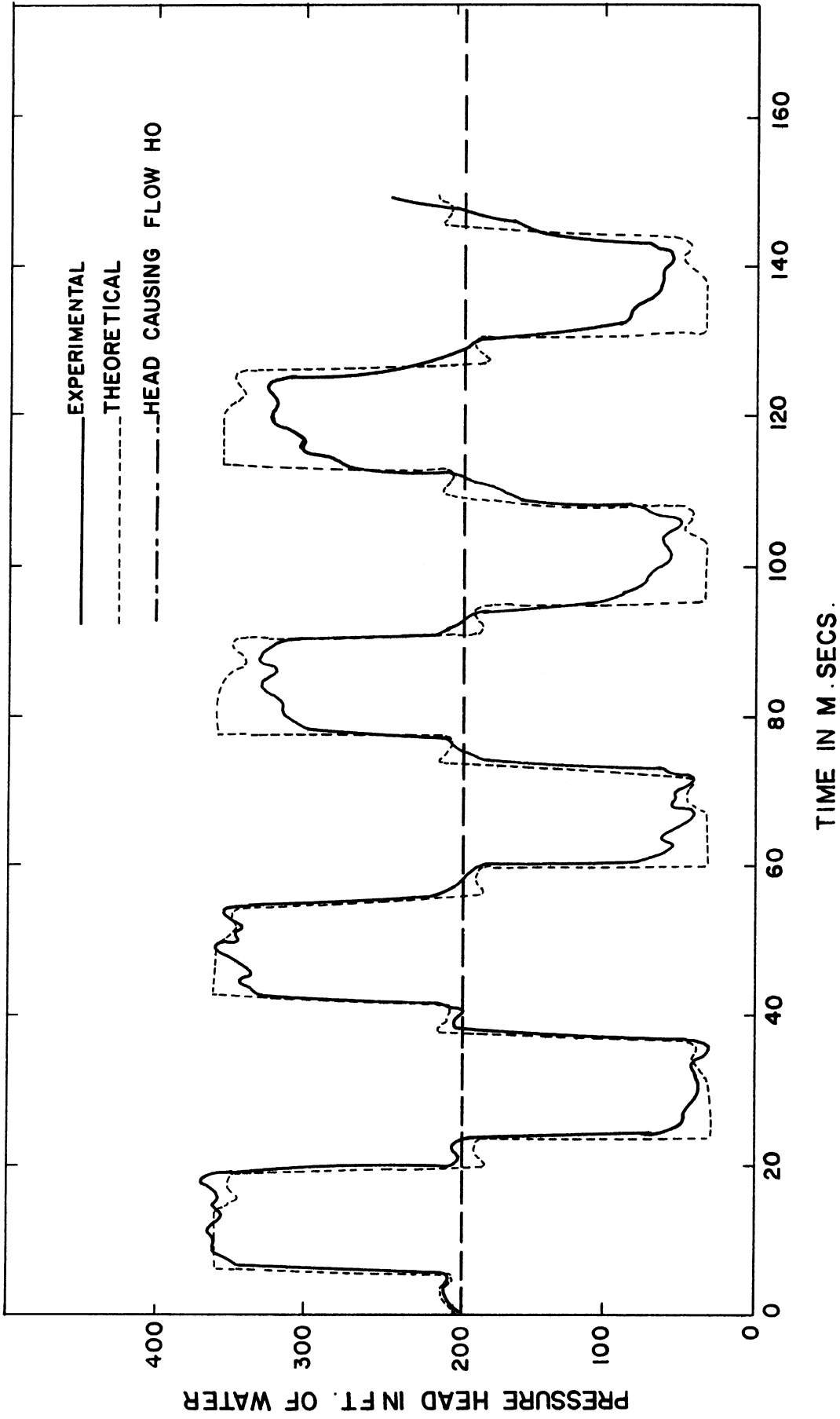
CASE 1(c)

Figure 18. Water-Hammer Pressure-Time Diagram. At $x = 31\frac{1}{4}$. Pipe with Minor Loss in Middle. Laminar Flow. $HO = 46.6'$; $VO = 0.300'$ /sec.; Temp. = $77^{\circ}F.$



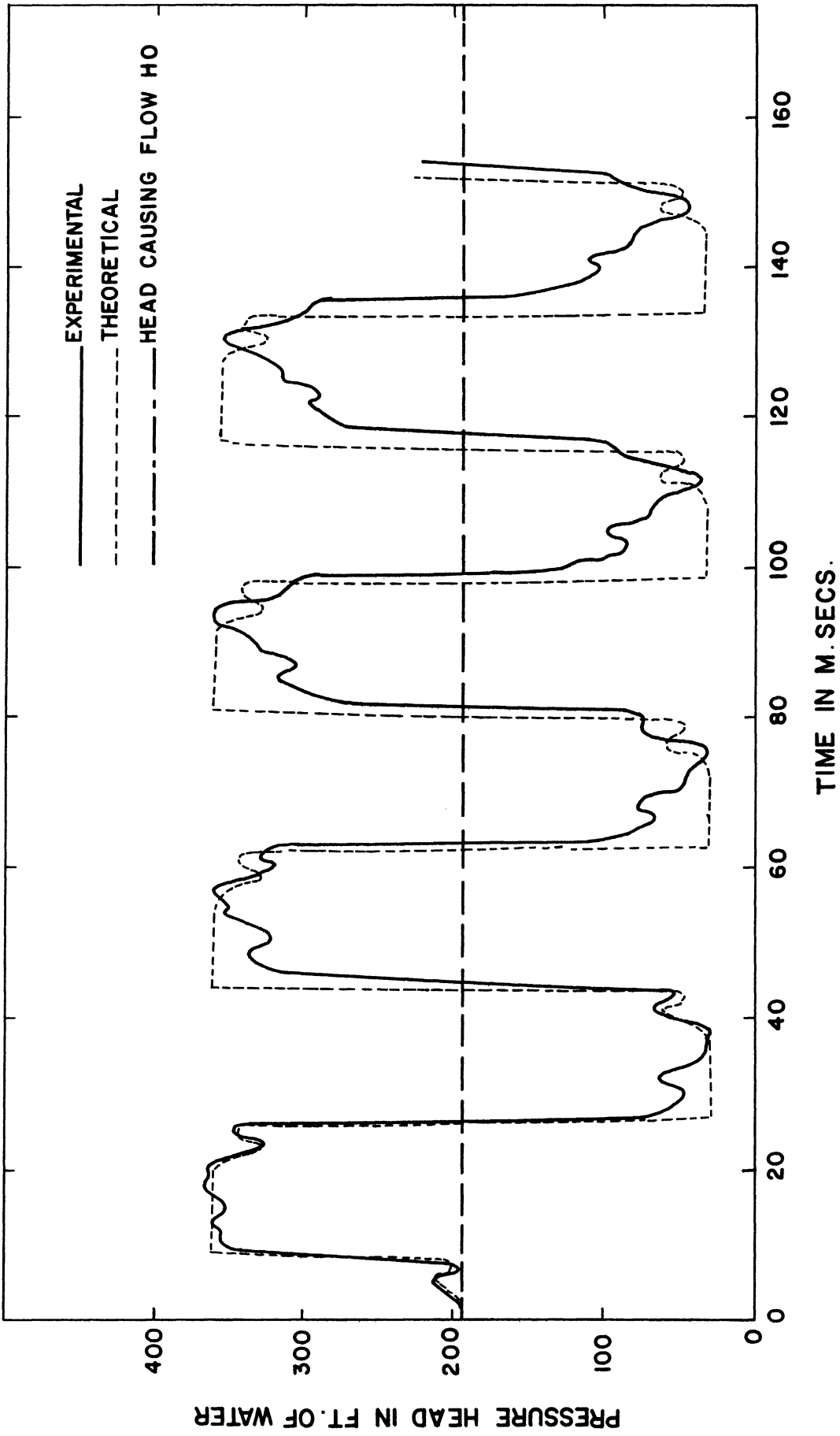
CASE 1(d)

Figure 19. Water-Hammer Pressure-Time Diagram. At $x = L$. Pipe with Minor Loss in Middle. Laminar Flow. $H_0 = 49.0'$; $V_0 = 0.350'$ /sec.; Temp. = 76°F .



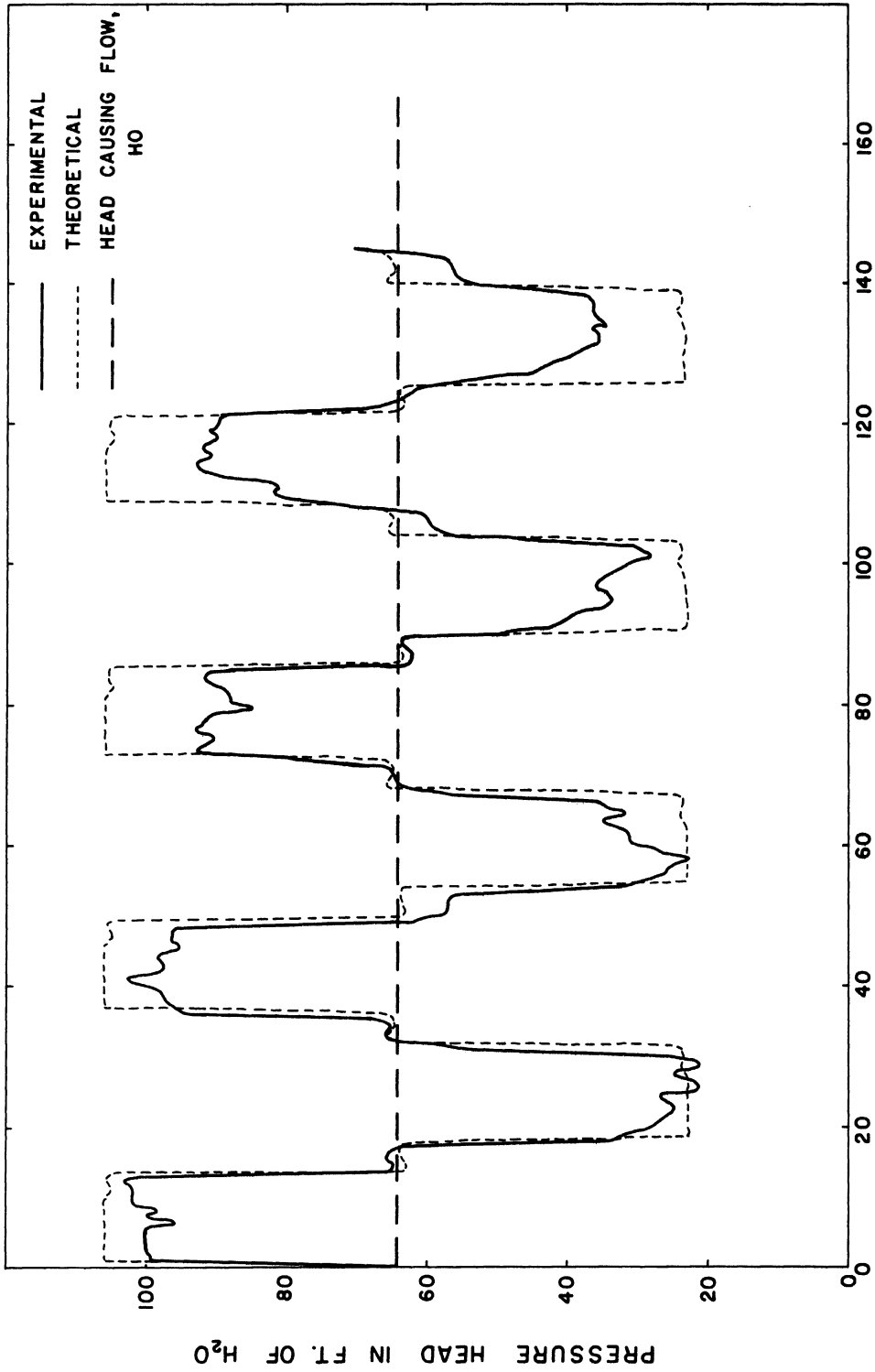
CASE 2(a)

Figure 20. Water-Hammer Pressure-Time Diagram. At $x = 3 \text{ I}/4$. Straight Pipeline; Turbulent Flow. $HO = 194.0$; $VO = 1.212 \text{ '}/\text{sec.}$; Temp. = 79°F.



CASE 2(b)

Figure 21. Water-Hammer Pressure-Time Diagram. At $x = L$ Straight Pipeline; Turbulent Flow. $H_0 = 194.0'$; $V_0 = 1.20'$ /sec.; Temp. $\approx 75^\circ\text{F}$.



TIME IN M. SECS.

CASE 2(c)

Figure 22. Water-Hammer Pressure-Time Diagram. At $x = 3L/4$ Straight Pipeline; Laminar Flow.

diagram that the theoretical program exactly depicts the experimental conditions.

When the pressure in the pipeline falls below the static head H_0 for the first time, air that was dissolved in the water at the static head H_0 , is liberated and begins to cushion the wave front. This effect can be seen in all of the remaining cycles, by the discrepancy which develops between the experimental and theoretical traces. This situation is more pronounced in the case of the pipeline with a minor loss than in the straight pipeline. This is so because the constriction at the orifices produces a far lower pressure than in the case of the straight pipeline and consequently, more dissolved air is set free.

There are several reasons to make one believe that the difference between the theoretical and experimental curves was due to gas liberation alone. First, the water used in the experiment was drawn from the sump in the laboratory. This water is far from pure as many additives are added for various purposes, such as rust-preventives and algae inhibitors. These compounds, like Chlorox and dilute Hydrochloric acid, when dissolved in water introduce gases like Chlorine, making the water more susceptible to gas liberation when subject to low pressures. Second, at the end of each experiment, bleeding of the pipeline at the orifice and at the valve would indicate the presence of small bubbles. Third, the discrepancy occurs only after the first drop in pressure below static pressure. The discrepancy cannot be attributed to an incorrect value of the steady-state loss coefficient or to the fact that the unsteady loss coefficient

was not used since the same type of discrepancy exists in the case of the straight pipeline. Finally, the nature of the discrepancy itself leads one to recognize it as one of air liberation. In nearly all the cases, air bubbles act as a spring cushioning the pressure change, allowing the maximum pressure to be reached after some time.

This phenomenon of air liberation could not be handled analytically because of several reasons. First, the mass of air set free would have to be determined by trial and error, and its distribution along the pipe length would also have to be assumed. Also, even if the above two factors were known, new equations would have to be developed to depict this phenomenon. The equations used for large air chambers^(3,16,59) would not be applicable in these circumstances for the following reason. Since the volume of air is so small, such large pressure changes are bound to produce heat, which would be dissipated in the water. This additional form of energy loss would have to be taken into account in the new equations. Because of these difficulties, the theoretical program did not take the effects of the liberated air into account.

Every care was taken to remove all the free air from the pipeline before the experiment began. However, it was impracticable to modify the experiment so that there was no air liberated from solution. Since a closed circuit was not feasible, use of distilled water would not have made any difference. It was also felt that use of an oil would not have helped, since most oils have volatile components which would vaporize at low pressures.

There are some diagrams in which the theoretical and experimental wave speeds differ. This discrepancy is believed due to errors in the sweep rate of the oscilloscope. It was found that there was a 6% error in the sweep rates of the oscilloscope. Calibration with an audio oscillator reduced the error to 1%, which error is noticeable in the traces.

For the case of laminar flow, it can be seen that the calculated and actual wave speeds do not differ by more than 1%. This is in contrast to the experimental results reported in Reference 78. The magnitude of the pressure wave also agrees fairly well with theoretical results, despite the assumption of uniform velocity distribution over the pipe area. However, it is not possible to see the reflection from the minor loss, because of the disturbances of the free air. A more elaborate theoretical study of waterhammer in laminar flow is presented by Rouleau.⁽⁷¹⁾ However, in the experimental verification of his theory he used oil flowing in a pipeline, and because of the volatile constituents of the oil, the experimental and theoretical traces did not match well.

IX. CONCLUSIONS

Whenever a water-hammer wave encounters a device causing a sharp energy loss, a reflection wave is sent back from it. The magnitude of this reflection is equal to $-\frac{\Delta(\text{MLOSS})}{2}$. The wave transmitted on is equal to the value of the approaching wave plus $\frac{\Delta(\text{MLOSS})}{2}$. Although the solution to the problem of a minor loss in a pipeline can be obtained graphically, it does not give one a clear idea of the mechanics of the problem.

The method of characteristics is a very simple and efficient way to provide particular solutions for the water-hammer equations, including friction effects. When setting up a computer program for water hammer in a pipeline with a minor loss in it, conditions at the minor loss must be treated as a boundary condition. The equations at the boundary condition verify the conclusions about the magnitude of the reflection wave, reached earlier. It is sufficiently accurate to use the steady-state loss coefficients of the device, at least for the case of instantaneous and rapid gate closures, even though water hammer is a markedly unsteady phenomenon.

An experiment conducted to verify the theoretical equations provided fairly good agreement between the experimental pressure diagram and the theoretical curve, thus validating the theory.

APPENDIX I

COMPUTER PROGRAM AND PRINT OUT FOR WATER HAMMER IN
A PIPELINE WITH A MINOR LOSS IN THE MIDDLE

004315 04/11/63 3 3 26.5 PM

\$. COMPILER MAD. EXECUTE

MAD (9 JAN 1963 VERSION) PROGRAM LISTING

WATERHAMMER IN A PIPE WITH A MINOR LOSS IN THE MIDDLE OF PIPE
LINE. CASE OF RAPID CLOSURE OF VALVE.
TIME OF CLOSURE TC=12.0MILLI SECS.
MINOR LOSS CREATED BY 3. ORIFICES. KOR=F(R).

READ DATA
PRINT COMMENT \$WATERHAMMER IN A PIPE WITH A MINOR LOSS IN TH
LE MIDDLE OF PIPELINE \$
PRINT COMMENT \$ CASE OF RAPID CLOSURE. TIME OF CLOSURE TC=12.
10 MILLI SECS.\$

PRINT COMMENT \$ MINOR LOSS CREATED BY 3. ORIFICES. KOR=F(R). \$
PRINT RESULTS HO,D,E,K1,8,N,L,NU,VO,TEMP,P,TC
INTERNAL FUNCTION (S)

ENTRY TO FR.
R=D*.ABS.(S*VO)/ZNU
WHENEVER R .L. 1.0
F=64.0
OR WHENEVER R .L. 2000.
F=64./R

OR WHENEVER R .L. 100000.
F=0.316/(R .P. 0.25)
END OF CONDITIONAL
FUNCTION RETURN F

END OF FUNCTION
INTERNAL FUNCTION (W)
ENTRY TO KOR.
R=D*.ABS.(W*VO)/ZNU
WHENEVER R .L. 250.
KORIF=1500.

OR WHENEVER R .L. 600.
KORIF=4700./ (R .P. 0.237)
OR WHENEVER R .L. 10000.
KORIF=1390./ (R .P. 0.0205)

END OF CONDITIONAL
FUNCTION RETURN KORIF
END OF FUNCTION
INTERNAL FUNCTION (I,LCOEF)

ENTRY TO BCOND.
C4=LCOEF*VO/ (8.*32.2*HO*BETA)
C5=(V(I-1)+V(I+2))/2.+(H(I-1)-H(I+2))/(4.*BETA)

1-L*VO*DELTA*(FR.(V(I-1))*V(I-1)+FR.(V(I+2))
2*V(I+2)*.ABS.V(I+2))/(2.*A*0)
VA=0.
WHENEVER LCOEF .G. 100000.
VP(I)=SQRT.(C5/C4-VA/C4)

OTHERWISE
VP(I)=C5-C4*VA*.ABS.VA
END OF CONDITIONAL
WHENEVER .ABS.(VP(I)-VA) .L. .ABS.(VA/200.), TRANSFER TO MES.
VA=VP(I)

TRANSFER TO MISS
VP(I+1)=VP(I)
MLOSS=LCOEF*VO*VP(I)*.ABS.VP(I)/(64.*HO)
HP(I)=BETA*(V(I-1)-V(I+2))-BETA*L*VO*DELTA*(FR.(V(I-1))*V(I-1))

FUNCTION STATEMENT
FOR FRICTION FACTOR

FUNCTION STATEMENT
FOR LOSS COEFFICIENT

FUNCTION STATEMENT
FOR MINOR LOSS
BOUNDARY CONDITION

*001
*002
*003
*004
*005
*006
*007
*008
*009
*010
*011
*012
*013
*014
*015
*016
*017
*018
*019
*020
*021
*022
*023
*024
*025
*026
*027
*028
*029
*030
*031
*032
*033
*034
*035
*036
*037
*038
*039
*040
*041
*042
*043
*044
*045

```

1*.ABS.V(I-1)-FR.(V(I+2))*V(I+2)+.ABS.V(I+2))/(A*D)+H(I-1)+H
2(I+2)/2+.MLOSS/2. *045
HP(I+1)=HP(I)-MLOSS *046
FUNCTION RETURN *047
END OF FUNCTION *048
A=SQRT(.132*2*K1/62.4)/(1.+(K1*D*0.92)/(E*B)) *049
DELX=L/N *050
DIMENSION V(100),H(100),VP(100),HP(100),EX(100),TAU(100) *051
INTEGER I,J,N,I,P *052
BETA=(A*VO)/(64.4*HO) *053
DEL=0.5/N *054
RO=D*VO/NU *055
DXFEET=L*DELX *056
DTSECS=DEL*2.*L/A *057
TCLOSE=IC*A/(2.*L) *058
PRINT RESULTS A, DELX,DELT,BETA,RO,DXFEET,DTSECS,TCLOSE *059
MLOSS=KOR.(VO)*VO*VO/(64.4*HO) *060
HLOSS=VO*VO/(11.04*HO) *061
KGV=64.4*HO/(VO*VO)-KOR.(VO)-[FR.(VO)]*L/D-62.0 *062
I=0. *063
J=0 *064
HF=FR.(VO)*L*VO*VO/(64.4*HO*N*D) *065
EX(0)=0. *066
HP(0)=1.0 *067
VP(0)=1.0 *068
THROUGH BOSTON, FOR I=1,1,I .G.P *069
VP(I)=1.0 *070
HP(I)=HP(I-1)-HF *071
EX(I)=EX(I-1)*DELX *072
WHENEVER I .E. 21 *073
HP(I)=HP(I)-MLOSS*HF *074
EX(I)=EX(I)-DELX *075
OR WHENEVER I .E. 42 *076
EX(I)=EX(I)-DELX *077
HP(I)=HP(I)+HF-MLOSS *078
END OF CONDITIONAL *079
CONTINUE *080
TIME=T*2.*L/A *081
PRINT RESULTS TIME,J,TAU(I) *082
PRINT FORMAT RESULT1,L*EX(0),L*EX(5),L*EX(10),L*EX(15), *083
L*EX(20),L*EX(21),L*EX(26),L*EX(31),L*EX(36),L*EX(41) *084
PRINT FORMAT RESULT2,HO*HP(0),HO*HP(5),HO*HP(10),HO*HP(15), *085
HO*HP(20),HO*HP(21),HO*HP(26),HO*HP(31),HO*HP(36),HO*HP(41) *086
PRINT FORMAT RESULT3,VO*VP(0),VO*VP(5),VO*VP(10),VO*VP(15), *087
VO*VP(20),VO*VP(21),VO*VP(26),VO*VP(31),VO*VP(36),VO*VP(41) *088
VECTOR VALUES RESULT1=$IH ,6H EX=10F10.2*$ *089
VECTOR VALUES RESULT2=$IH ,6H HEAD=10F10.4*$ *090
VECTOR VALUES RESULT3=$IH ,6H VEL.=10F10.4*$ *091
J=1 *092
T=J*DEL *093
TIME=T*2.*L/A *094
WHENEVER T.G.6.0, TRANSFER TO AOK *095
WHENEVER T .L. TCLOSE *096
THROUGH MYSCORE, FOR I=0,1,I.G.P *097
H(I)=HP(I) *098
V(I)=VP(I) *099
THROUGH NUYORK, FOR I=1,1,I.E.P *100
WHENEVER I.NE.20 .OR. I.NE.21 .OR. I.NE.41 .OR. I.NE.42 *101
HP(I)=(H(I+1)+H(I-1))/2.-BETA*(V(I+1)-V(I-1))+BETA*DEL *102
I(FR.(V(I+1))*ABS.V(I+1)+.ABS.V(I-1))-FR.(V(I-1))*ABS.V(I-1) *103

```

CALCULATION OF
CONSTANTS

INITIAL
CONDITIONS

```

21)) / (A*D)
VP(1) = (V(I-1) + V(I+1)) / 2 - (H(I-1) - H(I+1)) / (4 * BETA) - VO * L * DELT
1 * FR. (V(I-1) * V(I-1) * ABS. V(I-1) * V(I+1)) * FR. (V(I+1) * ABS. V(I+
21)) / (2 * A * D)
END OF CONDITIONAL
CONTINUE
HP(0) = 1.0
VP(0) = V(1) + (1. - H(1)) / (2 * BETA) - FR. (V(1)) * L * VO * DELT * V(1) * ABS.
1 * FR. (V(1) * ABS. V(1)) / (A * D)
K3 = KOR. (V(20))
EXECUTE BCND. (20, K3)
K3 = KOR. (VP(20))
EXECUTE BCND. (20, K3)
KSV = 62.0 / (TAU(J) * TAU(J))
EXECUTE BCND. (41, KSV)
C1 = KGV * VO * VD / (4 * 32 * 2 * HO * BETA)
C2 = L * VO * DELT * V(P-1) * ABS. V(P-1) * FR. (V(P-1)) / (A * D) - V(P-1) - (H
1 * FR. (V(P-1) * ABS. V(P-1)) / (2 * BETA)
VP(P) = (SORT. (1. - 4 * C2 * C1) - 1.) / (2 * C1)
WHENEVER VP(P) .LT. 0. .OR. VP(P) .GT. 1.01
C1 = -C1
VP(P) = (1. - SQRT. (1. - 4 * C2 * C1)) / (2 * C1)
END OF CONDITIONAL
HP(P) = KGV * VO * VP(P) * (1. - ABS. VP(P)) / (2 * 32 * 2 * HO)
PRINT RESULTS J, TIME, TAU(J)
PRINT FORMAT RESULT1, L * EX(0), L * EX(5), L * EX(10), L * EX(15),
L * EX(20), L * EX(25), L * EX(30), L * EX(35), L * EX(40), L * EX(45)
PRINT FORMAT RESULT2, HO * HP(0), HO * HP(5), HO * HP(10), HO * HP(15),
HO * HP(20), HO * HP(25), HO * HP(30), HO * HP(35), HO * HP(40), HO * HP(45)
PRINT FORMAT RESULT3, VO * VP(0), VO * VP(5), VO * VP(10), VO * VP(15),
VO * VP(20), VO * VP(25), VO * VP(30), VO * VP(35), VO * VP(40), VO * VP(45)
OTHERWISE
THROUGH BARODA, FOR I=0,1,1.G.41
H(I) = HP(I)
V(I) = VP(I)
THROUGH ANNARB, FOR I=1,1,1.E.41
WHENEVER I.NE.20 .OR. I.NE.21
HP(I) = (H(I+1) + H(I-1)) / 2 - BETA * (V(I+1) - V(I-1)) + BETA * VO * L * DELT *
1 * FR. (V(I+1) * V(I+1) * ABS. V(I+1)) - FR. (V(I-1) * V(I-1) * ABS. V(I-1)
21)) / (A * D)
VP(I) = (V(I-1) + V(I+1)) / 2 - (H(I+1) - H(I-1)) / (4 * BETA) - VO * L * DELT
1 * FR. (V(I-1) * V(I-1) * ABS. V(I-1) * V(I+1)) * FR. (V(I+1) * ABS. V(I+
21)) / (2 * A * D)
END OF CONDITIONAL
CONTINUE
HP(0) = 1.0
VP(0) = V(1) + (1. - H(1)) / (2 * BETA) - FR. (V(1)) * L * VO * DELT * V(1) * ABS.
1 * FR. (V(1) * ABS. V(1)) / (A * D)
K3 = KOR. (V(20))
EXECUTE BCND. (20, K3)
K3 = KOR. (VP(20))
EXECUTE BCND. (20, K3)
VP(41) = 0.
HP(41) = H(40) + 2 * BETA * V(40) - 2 * BETA * L * VO * FR. (V(40)) * DELT * V(40)
1 * ABS. V(40)) / (A * D)
PRINT RESULTS J, TIME
PRINT FORMAT RESULT1, L * EX(0), L * EX(5), L * EX(10), L * EX(15),
L * EX(20), L * EX(25), L * EX(30), L * EX(35), L * EX(40), L * EX(45)
PRINT FORMAT RESULT2, HO * HP(0), HO * HP(5), HO * HP(10), HO * HP(15),
HO * HP(20), HO * HP(25), HO * HP(30), HO * HP(35), HO * HP(40), HO * HP(45)
PRINT FORMAT RESULT3, VO * VP(0), VO * VP(5), VO * VP(10), VO * VP(15),
VO * VP(20), VO * VP(25), VO * VP(30), VO * VP(35), VO * VP(40), VO * VP(45)
END OF CONDITIONAL
J = J + 1
TRANSFER TO BOMBAY
CONTINUE
AOK
END OF PROGRAM
146
147
148
149

```

CALCULATION OF
V AND H FOR
TIME T LESS
THAN TC.

CALCULATION OF
V AND H FOR
TIME T GREATER
THAN TC.

THE FOLLOWING NAMES HAVE OCCURRED ONLY ONCE IN THIS PROGRAM.
COMPIATION WILL CONTINUE.

TEMP

WATERHAMMER IN A PIPE WITH A MINOR LOSS IN THE MIDDLE OF PIPELINE
CASE OF RAPID CLOSURE. TIME OF CLOSURE TC=12.0 MILLI SECS.
MINOR LOSS CREATED BY 3 DRIFICES. KOR-FIR.

HO =	46.600000	D =	0.440000	E =	2.450000E-09	K1 =	4.630000E-07
B =	4.040000E-03	N =	60	L =	60.000000	NU =	9.690000E-06
VO =	2.990000	TEMP =	77.000000	P =	61	IC =	0.120000
A =	4481.287122	DELX =	0.166667	DELI =	8.333333E-03	BETA =	446550
RO =	1357.688324	DXFEET =	1.000000	DISECS =	2.231153E-04	ICLOSE =	4448199
TIME =	0.000000	J =	0	TAU(0) =	1.000000		
EX =	5.00	10.00	15.00	20.00	20.00	25.00	30.00
HEAD =	46.6000	46.5751	46.5503	46.5254	46.5005	44.9289	44.9040
VEL =	2.990	2.990	2.990	2.990	2.990	2.990	2.990
J =	1	TIME =	2.231153E-04	TAU(1) =	0.997000		
EX =	5.00	10.00	15.00	20.00	20.00	25.00	30.00
HEAD =	46.6000	46.5751	46.5503	46.5254	44.8841	44.9040	44.8792
VEL =	2.990	2.990	2.990	2.987	2.987	2.990	2.990
J =	2	TIME =	4.462306E-04	TAU(2) =	0.993000		
EX =	5.00	10.00	15.00	20.00	20.00	25.00	30.00
HEAD =	46.6000	46.5751	46.5503	46.5254	44.8840	44.9040	44.8792
VEL =	2.991	2.991	2.991	2.987	2.987	2.991	2.991
J =	3	TIME =	6.693460E-04	TAU(3) =	0.992000		
EX =	5.00	10.00	15.00	20.00	20.00	25.00	30.00
HEAD =	46.6000	46.5751	46.5503	46.5254	44.8838	44.9040	44.8792
VEL =	2.991	2.991	2.991	2.988	2.988	2.991	2.991
J =	4	TIME =	8.924613E-04	TAU(4) =	0.989000		
EX =	5.00	10.00	15.00	20.00	20.00	25.00	30.00
HEAD =	46.6000	46.5751	46.5503	46.5254	44.8837	44.9040	44.8792
VEL =	2.991	2.991	2.991	2.988	2.988	2.991	2.991
J =	5	TIME =	1.115577E-03	TAU(5) =	0.985000		
EX =	5.00	10.00	15.00	20.00	20.00	25.00	30.00
HEAD =	46.6000	46.5751	46.5503	46.5254	44.8836	44.9040	44.8792
VEL =	2.991	2.991	2.991	2.988	2.988	2.991	2.991
J =	6	TIME =	1.338692E-03	TAU(6) =	0.980000		
EX =	5.00	10.00	15.00	20.00	20.00	25.00	30.00
HEAD =	46.6000	46.5751	46.5503	46.5254	44.8834	44.8599	44.8792
VEL =	2.992	2.992	2.988	2.988	2.988	2.992	2.991
J =	7	TIME =	1.561807E-03	TAU(7) =	0.975000		
EX =	5.00	10.00	15.00	20.00	20.00	25.00	30.00
HEAD =	46.6000	46.5751	46.5503	46.5254	44.8833	44.8598	44.8792
VEL =	2.992	2.992	2.989	2.989	2.989	2.989	2.992
J =	8	TIME =	1.784923E-03	TAU(8) =	0.970000		
EX =	5.00	10.00	15.00	20.00	20.00	25.00	30.00
HEAD =	46.6000	46.5751	46.5503	46.5254	44.8832	44.8597	44.8792
VEL =	2.992	2.992	2.989	2.989	2.989	2.989	2.992
J =	9	TIME =	2.006803E-03	TAU(9) =	0.960000		

APPENDIX II

COMPUTER PROGRAM AND PRINT OUT OF WATER HAMMER
IN A STRAIGHT PIPELINE

MAD (9 JAN 1963 VERSION) PROGRAM LISTING

WATERHAMMER IN A STRAIGHT PIPELINE
CASE OF RAPID CLOSURE OF VALVE. TIME OF CLOSURE=12.0 M. SECS.

PRINT COMMENT \$1 WATERHAMMER IN A STRAIGHT PIPELINE \$ *001
PRINT COMMENT \$ CASE OF RAPID CLOSURE. TIME OF CLOSURE. TC=12. *002
IC MILLI SECS. \$ *003

READ DATA *004

PRINT RESULTS HO,D,E,K1,B,N,L,NU,VO,TEMP,P,TC *005

INTERNAL FUNCTION (S) *006

ENTRY TO FR. *007

R=D*.ABS.(S*VO)/NU *008

WHENEVER R.L.I.0 *009

F=64. *010

OR WHENEVER R .L. 2000. *011

F=64./R *012

OR WHENEVER R .L. 100000. *013

F=C.316/IR .P. 0.25) *014

END OF CONDITIONAL *015

FUNCTION RETURN F *016

END OF FUNCTION *017

INTERNAL FUNCTION (I,LCOEF) *018

ENTRY TO BCOND. *019

C4=LCOEF*VO*VO/(8.*32-2*HO*BETA) *020

C5=(V(I-1)+V(I+2))/2+(H(I-1)-H(I+2))/(4.*BETA) *021

1-L*VO*DELTA*(FR.(V(I-1)+V(I+2))-ABS.V(I-1)+FR2.(V(I+2))) *022

2*V(I+2)*ABS.V(I+2))/(2.*A*D) *023

VA=0. *024

WHENEVER LCOEF .G. 100000. *025

VP(I)=SQRT.(C5/C4-VA/C4) *026

OTHERWISE *027

VP(I)=C5-C4*VA*ABS.VA *028

WHENEVER .ABS.(VP(I)-VA) .L. .ABS.(VA/200.), TRANSFER TO HES *029

VA=VP(I) *030

TRANSFER TO MISS *031

VP(I+1)=VP(I) *032

MLOSS=LCOEF*VO*VO*VP(I)*ABS.VP(I)/(164.4*HO) *033

HP(I)=BETA*(V(I-1)-V(I+2))-BETA*L*VO*DELTA*(FR.(V(I-1)+V(I+2))) *034

1*ABS.V(I-1)-FR.(V(I+2))*V(I+2)*ABS.V(I+2)/(A*D) +(H(I-1)+H *035

2(I+2))/2.+MLOSS/2. *036

HP(I+1)=HP(I)-MLOSS *037

FUNCTION RETURN *038

END OF FUNCTION *039

A=SQRT.(132-2*K1/62.4)/(1.+(K1*0.92)/(E*8))) *040

DIMENSION V(100),H(100),VP(100),HP(100),EX(100),TAU(100) *041

DELX=I./N *042

INTEGER I,J,N,P *043

BETA=(A*VO)/(164.4*HO) *044

DELTA=C.5/N *045

RO=D*VO/NU *046

DXFEET=L*DELX *047

DTSECS=DELTA*2.*L/A *048

TGCLOSE=TC*A/(2.*L) *049

PRINT RESULTS A, DELX, DELTA, BETA, RO, DXFEET, DTSECS, TGCLOSE *050

FUNCTION STATEMENT

FOR PIPE FRICTION

FACTOR

FUNCTION STATEMENT

FOR MINOR LOSS

BOUNDARY CONDITION

CALCULATION OF

CONSTANTS

```

HLDS5=VO*VO/(1.04*HD)
KGV=2.*32.2*HD/(VO*VO)- (FR.(VO))*L/D-62.0
I=0.
J=0
MF=FR.(VO)*L*VO*VO/(64.*HD*N*D)
EX(0)=0.
HP(0)=1.0
VP(0)=1.0
THROUGH BOSTON, FOR I=1,1,I .G.P
VP(I)=1.0
HP(I)=HP(I-1)-HF
EX(I)=EX(I-1)+DELX
WHENEVER I.E.41
EX(I)=EX(I)-DELX
HP(I)=HP(I)+HF-HLOSS
END OF CONDITIONAL
CONTINUE
TIME=T*2.*L/A
PRINT RESULTS J,TIME,TAU(J)
PRINT FORMAT RESULT1,L*EX(0),L*EX(5),L*EX(10),L*EX(15),
LL*EX(20),LL*EX(25),L*EX(30),L*EX(35),L*EX(40)
PRINT FORMAT RESULT2,HO*HP(0),HO*HP(5),HO*HP(10),HO*HP(15),
HO*HP(20),HO*HP(25),HO*HP(30),HO*HP(35),HO*HP(40)
PRINT FORMAT RESULT3,VO*VP(0),VO*VP(5),VO*VP(10),VO*VP(15),
VO*VP(20),VO*VP(25),VO*VP(30),VO*VP(35),VO*VP(40)
VECTOR VALUES RESULT1=$IH ,6H EX=9F10.2**$
VECTOR VALUES RESULT2=$IH ,6H HEAD=9F10.4**$
VECTOR VALUES RESULT3=$IH ,6H VEL.=9F10.4**$
J=1
I=J*DEL T
WHENEVER I.G.6.0,TRANSFER TO AOK
WHENEVER T .L. TCLOSE .AND. TAU(J) .G. 0.01
THROUGH MYSCORE, FOR I=0,1,I.G.P
H(I)=HP(I)
V(I)=VP(I)
THROUGH NU York, FOR I=1,1,I.E.P
WHENEVER I.NE.40 .OR. I.NE.41
HP(I)=(H(I+1)+H(I-1))/2.-BETA*(V(I+1)-V(I-1))+BETA*VO*L*DEL T*
1(FR.(V(I+1))*V(I+1)*ABS.V(I+1)-FR.(V(I-1))*V(I-1)*ABS.V(I-1
2))/A*0)
VP(I)=(V(I+1)+V(I-1))/2.- (H(I+1)-H(I-1))/(4.*BETA)-VO*L*DEL T
1*(FR.(V(I-1))*V(I-1)*ABS.V(I-1)+V(I+1)*FR.(V(I+1))*ABS.V(I+
2))/A*0)
END OF CONDITIONAL
CONTINUE
HP(0)=1.0
VP(0)=V(I)+(HP(0)-H(I))/(2.*BETA)-L*VO*DEL T*FR.(V(I))*V(I)*
1.ABS.V(I)/A*0)
TIME=T*2.*L/A
KSV=62.0/(TAU(J)*TAU(J))
EXECUTE BCOND.(40,KSV)
C1=KGV*VO*VO/(4.*32.2*HD*BETA)
C2=L*VO*DEL T*V(P-1)*ABS.V(P-1)*FR.(V(P-1))/(A*0)-V(P-1)-IH
1(P-1)/(2.*BETA)
WHENEVER (1.-4.*C2*C1)-L.0., C1=-C1
VP(P)=(SORT(1.-4.*C2*C1)-1.)/(2.*C1)
HP(P)=KGV*VO*VO*VP(P)*L.ABS.V(P))/L*32.2*HD)
PRINT RESULTS J,TIME,TAU(J)
PRINT FORMAT RESULT1,L*EX(0),L*EX(5),L*EX(10),L*EX(15),
LL*EX(20),LL*EX(25),L*EX(30),L*EX(35),L*EX(40)

```

INITIAL CONDITIONS

CALCULATION OF V AND H FOR TIME T LL THAN TC.

*047
*048
*049
*050
*051
*052
*053
*054
*055
*056
*057
*058
*059
*060
*061
*062
*063
*064
*065
*066
*067
*068
*069
*070
*071
*072
*073
*074
*075
*076
*077
*078
*079
*080
*081
*081
*082
*082
*083
*084
*085
*086
*087
*088
*089
*090
*091
*092
*093
*094
*095
*096
*096


```

PRINT_FORMAT_RESULT2,HO*HP(10),HO*HP(15),HO*HP(10),HO*HP(15),
1HO*HP(20),HO*HP(25),HO*HP(30),HO*HP(35),HO*HP(40)
PRINT_FORMAT_RESULT3,VO*VP(10),VO*VP(15),VO*VP(10),VO*VP(15),
1VO*VP(20),VO*VP(25),VO*VP(30),VO*VP(35),VO*VP(40)
OTHERWISE
THROUGH BARODA, FOR I=0,1,6.40
H(I)=HP(I)
V(I)=VP(I)
THROUGH ANNARB, FOR I=1,1,6.40
HP(I)=(H(I+1)+H(I-1))/2.-BETA*(V(I+1)-V(I-1))+BETA*VO*L*DELTA
1FR,IV(I+1),Y(I+1),ABS,V(I+1)-FR,IV(I-1),Y(I-1),ABS,V(I-1
2))/L*A*0
VP(I)=(V(I+1)+V(I-1))/2.-H(I+1)-H(I-1)/(L*BETA)-VO*L*DELTA
1*(FR,IV(I+1),Y(I+1),ABS,V(I+1)-FR,IV(I+1),Y(I+1),ABS,V(I+
2))/L*A*0
HP(0)=1.0
VP(0)=V(I)+HP(0)-H(I)/(2.*BETA)-L*VO*DELTA*FR,IV(I),Y(I)*
1,ABS,V(I)/L*A*0
VP(40)=0.
HP(40)=H(39)+2.*BETA*V(39)-2.*BETA*L*VO*FR,IV(39),Y(39)*DELTA*V(39)
1*(ABS,V(39))/L*A*0
TIME=T*2.*L/A
PRINT_RESULTS,J,TIME
PRINT_FORMAT_RESULT1,L*EX(0),L*EX(5),L*EX(10),L*EX(15),
1L*EX(20),L*EX(25),L*EX(30),L*EX(35),L*EX(40)
PRINT_FORMAT_RESULT2,HO*HP(0),HO*HP(5),HO*HP(10),HO*HP(15),
1HO*HP(20),HO*HP(25),HO*HP(30),HO*HP(35),HO*HP(40)
PRINT_FORMAT_RESULT3,VO*VP(0),VO*VP(5),VO*VP(10),VO*VP(15),
1VO*VP(20),VO*VP(25),VO*VP(30),VO*VP(35),VO*VP(40)
END OF CONDITIONAL
J=J+1
TRANSFER TO BOMBAY
CONTINUE
END OF PROGRAM

```

**CALCULATION OF
V AND H FOR
TIME T GREATER
THAN TC.**

ADK

THE FOLLOWING NAMES HAVE OCCURRED ONLY ONCE IN THIS PROGRAM.
COMPILATION WILL CONTINUE.

TEMP

BIBLIOGRAPHY

1. Allievi, L. "Teoria Generale del Moto Perturbato dell'acqua nei Tubi in Pressione." Annali della Societa degli Ingegneri ed Architetti Italiani, Milan, 1903.
2. Theory of Water Hammer. Translated by E. E. Halmos. Printed by Ricardo Garoni, Rome, Italy, 1925.
3. "Air Chambers for Discharge Pipes." Trans. ASME (1937), 651.
4. Angus, R. W. "Simple Graphical Solution for Pressure Rise in Pipes and Pump Discharging Lines." The Engineering Journal, 18 (1935), 72.
5. "Kreitner's Diagram for Water Hammer Problems." Mech. Engrg. (1935), 781.
6. "Water Hammer in Pipes Including Those Supplied by Centrifugal Pumps - Graphical Treatment." Proc., Institute of Mech. Engrgs., 136 (1937), 245.
7. "Air Chambers and Valves in Relation to Water Hammer." ASME Trans. (1937), 661.
8. "Water Hammer Pressures in Compound and Branched Pipes." ASCE. Trans., 104 (1939), 340.
9. Arden, B., Galler, B. and Graham, R. Michigan Algorithm Decoder. The University of Michigan, Ann Arbor, Michigan, 1960.
10. Ball, E. B. "Methods Employed to Remedy Water-Hammer Shock in Pumping Systems." ASME, Trans. (1939), 5.
11. Barbarosa, N. L. "Hydraulic Analysis of Surge Tanks by Digital Computer." ASCE. Proc., Jour. of Hyd. Div., No. HY4, April, 1959.
12. Bergeron, L. "Etude des Variations de Regime dans les Conduites d'eau." Revue Generale de l'Hydraulique, Paris, 1 (1935), 12.
13. Du Coup de Belier en Hydraulique au Coup de Foudre en Electricite. Dunod, Paris, 1950.
14. Binnie, A. M. "The Effect of Friction on Surges in Long Pipelines." Quarterly Jour. of Mech. and Applied Maths., IV, Part 3 (1951), 330.
15. Bratfisch, A. E. and Cartwright, K. O. "Water Hammer Calculations and Test Results - Owens George Power Plant Penstocks." ASME Trans. (1956), 1329.

16. Calame, J. and Gaden, D. Theorie des Chambres d'Equilibre. Gauthur-Villars, Paris, 1926.
17. Creager, W. P. and Justin, J. D. Hydroelectric Handbook. John Wiley and Sons, Inc., New York, 2nd. Ed.
18. Daily, J. W. and Hankey, W. L., Jr. Resistance Coefficients for Accelerated Flow through Orifices. Tech. Rep. No. 10, Hydrodynamics Lab., Massachusetts Institute of Technology.
19. Daily, J. W. and Jordaan, J. M., Jr. Effects of Unsteadiness on Resistance and Energy Dissipation. Tech. Rep. No. 22, M.I.T. Hydrodynamics Lab.
20. Dawson, F. M. and Kalinske, A. A. "Methods of Calculating Water Hammer Pressures." Jour. A.W.W.A., 31 (1939), 1835.
21. Durand, W. F. "Application of Law of Kinematic Similitude to Surge Chamber Problem." ASME Trans. (1921), 1177.
22. "Control of Surges in Water Conduits." ASME Trans. (1912), 319.
23. Evans, W. E. and Crawford, C. C. "Design Charts for Air Chambers on Pump Lines." ASCE Trans., 119 (1954), 1025.
24. Ezekiel, F. D. and Paynter, H. M. "Firmoviscous and Anelastic Properties of Fluids and Their Effects on the Propagation of Compression Waves." ASME (1959), Paper No. 59, Hyd-19.
25. Gibson, W. L. and Shelson, W. "Experimental and Analytical Investigation of a Differential Surge Tank Installation." ASME Trans. (1956), 925.
26. Gray, C. A. M. "Analysis of Water Hammer by Characteristics." ASCE Trans., 119 (1954), 1176.
27. "The Dissipation of Energy in Water Hammer." Australian Journal of Applied Science (June, 1954), 125.
28. de Haller, P. and Bedue, A. "The Break-away of Water Columns as a Result of Negative Pressure Shocks." Water and Water Engrg., 56 (June, 1952), 220.
29. Halliwell, A. R. "Velocity of a Water-Hammer Wave in an Elastic Pipe." Jour. of the Hydraulics Div., Proc. of the ASCE, 89, No. Hy4, July, 1963.
30. Jacobson, R. S. Charts for Analysis of Surge Tanks in Turbine and Pump Installations. Special Report No. 104, Bureau of Reclamation, Feb., 1952.

31. Jaeger, C. "Theory of Resonance in Pressure Conduits." ASME Trans, 61 (1939), 109.
32. "Water-Hammer Effects in Power Conduits." Civil Engrg. and Public Works Review, 1948.
33. "The Double Surge Tanks Systems." Water Power, 9 (July, 1957), 253; (Aug., 1957), 301.
34. "Contribution to the Stability Theory of Systems of Surge Tanks." ASME Trans., 80 (1958), 1574.
35. Johnson, R. D. "Surge Tanks in Water Power Plants." ASME Trans. (1908), 443.
36. Joukowsky, N. "Ueber den Hydraulischen Stoss in Wasserleitungsrohren." Memoires de l'Academic des Sciences de St. Petersburg, IX, 8 e Serie, 1898.
37. "Water Hammer." Translated by Miss O. Simin, Proc. A.W.W.A., 24 (1904), 341-424.
38. Kephart, J. T. and Davis, K. "Pressure Surges Following Water-Column Separation." ASME Trans., 83D., Jour. of Basic Engrg. (Sept., 1961), 456-460.
39. Kennison, H. F. "Surge-Wave Velocity -- Concrete Pressure Pipe." ASME Trans. (1956), 1323.
40. Kerr, S. L. "Fall in Pressure in Hydraulic Turbine Penstocks Due to Acceleration of Flow." Power, 60, No. 7 (Aug., 1924), 266-268.
41. "New Aspects of Maximum Pressure Rise in Closed Conduits." ASME Trans (1929), Hyd-51-3.
42. "Hydraulic Surges in Pump Discharge Lines." Proc. National Conference of Industrial Hydraulics, II (1948), 94-104.
43. "Surge Problems in Pipe Lines -- Oil and Water." Trans. ASME (1950), 667.
44. "Practical Aspects of Water Hammer." Jour. A.W.W.A., 40 (1958), 599.
45. Kerr, S. L., Kessler, L. H. and Gamet, M.B. "New Method for Bulk-Modulus Determinations." Trans. ASME (1950), 1143.
46. Kersten, R. D. and Walker, E. J. "Predicting Surge Pressures in Oil Pipelines." ASCE Trans., 124 (1959), 258.

47. Kessler, L. H. "Speed of Water-Hammer Pressure Wave in Transit Pipe." ASME Trans. (1939), 11; Discussion Trans. (1939), 451.
48. Kittredge, C. P. "Hydraulic Transients in Centrifugal Pump Systems." Trans. ASME (1956), 1307.
49. Knapp, F. "Operation of Emergency Shutoff Valves in Pipe Lines." ASME Trans. (1937), 679; Discussion Trans. (1939), 75.
50. Knapp, R. T. "Complete Characteristics of Centrifugal Pumps and Their Use in the Prediction of Transient Behaviour." ASME Trans., 59, Paper Hyd-59-11 (Nov., 1937), 683-689.
51. Le Conte, J. N. "Experiments and Calculations of Resurge Phase of Water Hammer." ASME Trans. (1937), 691; Discussion Trans. (1939), 440.
52. Li, Wen-Hsiung. "Mechanics of Pipe Flow Following Column Separation." ASCE, Jour. of Engrg. Mech., 88 (Aug., 1962), 97.
53. Lister, M. "The Numerical Solutions of Hyperbolic Partial Differential Equations by the Method of Characteristics." Chapter in, Mathematical Methods for Digital Computers, Edited by Ralston, A. and Wilf, H. S. John Wiley and Sons, Inc., 1960.
54. McCaig, I. W. and Jonker, F. H. "Applications of Computer and Model Studies to Problems Involving Hydraulic Transients." ASME, Jour. of Basic Engrg., 81 (1959), 433.
55. McNowen, J. S. "Surges and Water Hammer." Chapter in, Engineering Hydraulics, Edited by H. Rouse. John Wiley and Sons, Inc., New York, 1950.
56. Michaud, J. Coup de belier dans les conduites. Bull. de la Soc. vaudoise des Ing. et Arch. Lausanne, 1878.
57. Parmakian, J. "Pressure Surge Control at Tracy Pumping Plant." Proc. ASCE, 79 (Dec., 1953), Separate No. 361.
58. "Pressure Surges in Pump Installations." ASCE Trans., 120 (1955) 697.
59. Water-Hammer Analysis. Prentice-Hall Inc., New York, 1955.
60. "Water Hammer Design Criteria." Proc. ASCE (Apr., 1957), Paper 1216 in Power Journal.
61. "One-way Surge Tanks for Pumping Plants." ASME Trans., 80 (1958), 1563.
62. Paynter, H. M. and Ezekiel, F. D. "Water Hammer in Non-uniform Pipes as an Example of Wave Propagation in Gradually Varying Media." ASME Trans., 80 (1958), 1585.

63. Peabody, R. M. "Typical Analysis of Water Hammer in Pumping Plant of Colorado River Aqueduct." ASME Trans. (1939), 117.
64. Quick, R. S. "Comparison and Limitations of Various Water-Hammer Theories." Mech. Engrg. (1927), 524; Discussion Mech. Engrg. (1927), 1219.
65. "Development of Water Hammer Theory and Its Applications." Mech. Engrg. (1930), 376.
66. Rich, G. R. "Water-Hammer Analysis by the Laplace-Mellin Transformation." ASME Trans. (1945), 361.
67. "Basic Hydraulic Transients." Jour. of Boston Society of Civil Engrgs., 1948.
68. "Hydraulic Transients." 1st Ed. Engineering Societies Monographs. McGraw-Hill Book Co., Inc., New York, 1951.
69. "Water Hammer." Chapter in Handbook of Hydraulics. Edited by Davis, C. V., 2nd Edition, McGraw-Hill Book Co., Inc., New York, 1951.
70. Richards, R. T. "Water Column Separation in Pump Discharge Lines." ASME Trans. (1956), 1297.
71. Rouleau, W. T. "Pressure Surges in Pipelines Carrying Viscous Liquids." ASME, Jour. of Basic Engrg. (Dec., 1960), 912-920.
72. Schnyder, O. "Comparisons Between Calculated and Test Results on Water Hammer in Pumping Plants." ASME Trans. (1937), 695.
73. Schoklitsch, A. "Hydraulic Structures." ASME Trans., II (1937), 867-883. Translation.
74. Skalak, R. "An Extension of the Theory of Water Hammer." ASME Trans. (1956), 105.
75. Stepanoff, A. J. "Elements of Graphical Solution of Water-Hammer Problems in Centrifugal Pump Systems." ASME Trans. (1949), 515.
76. Streeter, V. L. Fluid Mechanics. McGraw-Hill Book Co., Inc., New York, 1958.
77. "Valve Stroking to Control Water Hammer." Jour. of the Hydraulics Div., Proc. of the ASCE, 89, No. Hy2, Mar. 1963.
78. Streeter, V. L. and Lai, Chintu. "Water-Hammer Analysis Including Fluid Friction." ASCE Proc., Paper 3135, May, 1962.

79. Strowger, E. B. "Relation of Relief Valve and Turbine Characteristics In Determination of Water Hammer." ASME Trans. (1937), 701; Discussion Trans. (1938), 608.
80. "Water-Hammer Problems in Connection with the Design of Hydro-Electric Plants." ASME Trans. (1945), 377.
81. Symposium on Water Hammer. ASME - ASCE, 1933.
82. Walker, M. L., Kirkpatrick, E. T. and Rouleau, W. T. "Viscous Dispersion in Water Hammer." ASME Trans. Jour. of Basic Engrg., 82, (Dec., 1960), 759-763.
83. White, I. M. "Application of the Surge Suppressor in Water Systems." Water Works Engrg., March 25, 1942.
84. Wood, F. M. "Application of Heaviside's Operational Calculus to Solution of Problems in Water Hammer." ASME Trans. (1937), 707; Discussion Trans. (1938), 682.

UNIVERSITY OF MICHIGAN



3 9015 02841 2776